Application of amorphous sugar matrix dried from alcohol to solid dispersion of hydrophobic drug and its physicochemical characteristics

アルコールから乾燥調製した糖類アモルファスマトリクスの難水溶性薬剤の固体分散キャリアとしての応用とその物理化学的特性

September, 2023

Koji Takeda

Graduate School of

Natural Science and Technology

(Doctor's Course)

OKAYAMA UNIVERSITY

Contents

Chapter 1 General Introduction

1.1. Sugar in Amorphous State

"Sugar" is an indispensable and ubiquitous material in pharmaceutical and food industries. Dissolved form of sugar is used as sweetener and/or thickener for liquid products including beverage and liquid medicine, and crystalline state of sugar serves as sweetener, nutrition, and/or bulk forming agents in the solid food and pharmaceutical products. On the other hand, sugars in the amorphous state are also included, more or less, in solidified or dried form of food and pharmaceutical products. The amorphous phase of sugar has a prominent structural flexibility and thus can an embed a wide range of substances stably and flatly. Therefore, the amorphous sugar phase in food and pharmaceutical products play important roles in holding functional components such as flavoring substance, nutrition, taste components, etc, as well as in moisture retaining and textures. Furthermore, the amorphous structure, comprised of sugar, has been preferably utilized as an excipient and a stabilizing agent in the drug industries (Manning et al., 1989; Pikal, 1994) and essential ingredients in many foods (Slade & Levine, 1993; White & Cakebread, 1996.).

In spite of the superiority of amorphous state of sugar, as described above, the pathways of amorphization of sugar is limited to only two. One is to dissolve sugar in water, together with other food or pharmaceutical ingredient, and dehydrate the aqueous solution of sugar under an appropriate condition. The other is to melt the crystalline sugar and mixed with the functional substances, followed by solidifying by quench cooling. These two pathways for sugar-amorphization are based on high solubility of sugar in solvent water and the compatibility of the functional substances with (hydrophilic) sugar, respectively. Accordingly, it has followed that the substances/materials, able to be embedded in amorphous sugar, are restricted to hydrophilic ones.

1.2. Novel Pathway of Sugar Amorphization Based on Over-Dissolution of Sugar in Alcohol

It is generally accepted that sugars could not dissolve in organic solvent, including alcohols. However, if sugar is amorphized and dispersed in an alcohol, it eventually

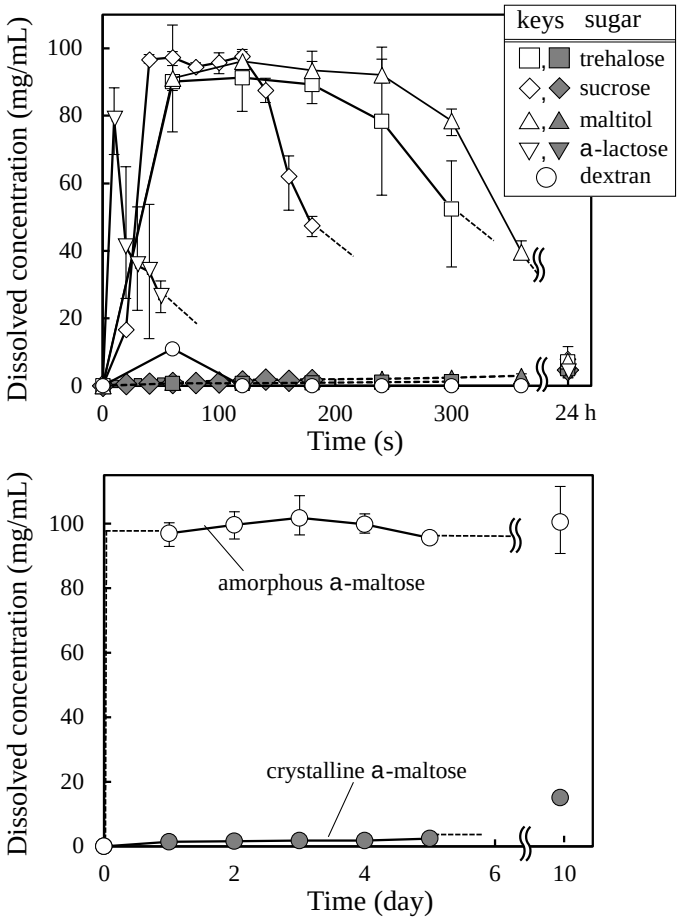

Fig. 1.2.1. Dissolution profiles of freeze-dried amorphous sugars (open keys) and crystalline ones (gray keys) in methanol. Amorphous sugar cake (1 g) was added to methanol (10 mL) and the resulting mixture was stirred at 200 rpm with a 1.5-cm magnetic stirring bar throughout the dissolution experiment. Error bars represent the highest and lowest values obtained for each condition. (Satoh et al., 2016)

become dissolved in that solvent even for a short period of time (Patent No. 6524744). Representative time courses (Satoh et al., 2016) for the concentration of dissolved sugar in methanol are shown in Fig. 1.2.1. In most cases except for dextran, freeze-dried sugar cakes appear to be fully dissolved in methanol soon after being suspended in methanol (Fig. 1.2.1). The dissolved concentration of sugar usually then decreases to the equilibrium values while the concentrations for crystalline sugars were quite low from first to last as well known. These clearly demonstrate that the over-dissolution of sugar into organic solvent occurs by the amorphization. Actually, Flores et al. (2002) reported that amorphized sucrose was enzymatically esterified with fatty acids in an organic media to a greater extent than the crystalline compound by increasing the concentration of

sucrose in the mixture.

Here, by using the over-dissolution of sugar in alcohol, the following novel sugar-amorphization technique has been developed (Patent No. 6524744) (Fig. 1.2.2): (i) Sugar is amorphized somehow such as by freeze-drying an aqueous solution and (ii) added to

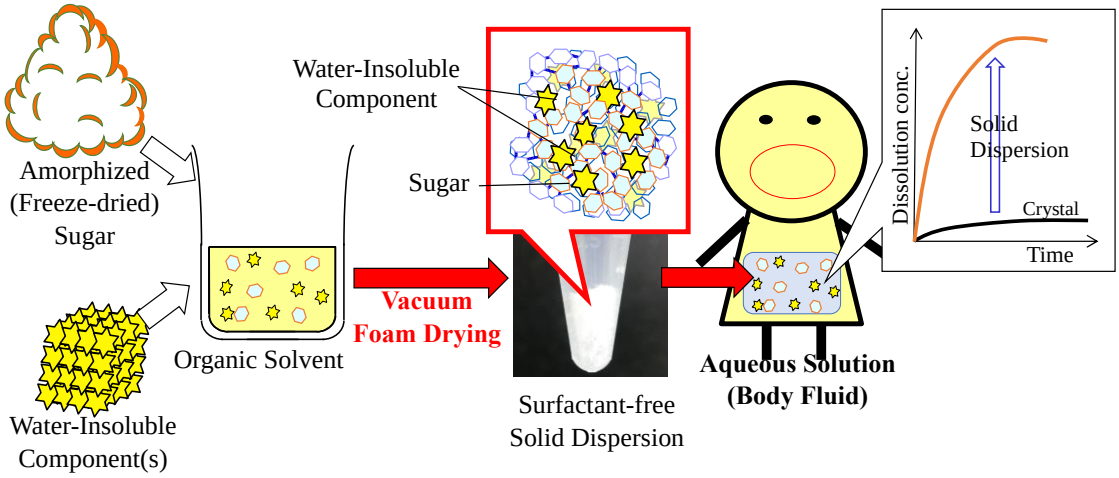

Fig. 1.2.2. Surfactant-free solid dispersion of water-insoluble drugs, based on the over-dissolution of sugar in organic solvent

an organic solvent, followed by homogenization. (iii) The homogenized solution is then dried before the segregation and crystallization of sugar occurs. It has been revealed that some types of sugar such as a-maltose could be dried from methanol without any crystallization (Satoh et al., 2016). However, it has not been unclear even whether the alcohol-originated amorphous sugar is different in the physicochemical characteristics from the normal water originated ones or not. In the Section 1.5, I review the reports and the existing findings on the physicochemical characteristics of amorphous sugar that had been obtained through the authentic methods.

1.3. Application of Alcohol-Originated Amorphous Sugar Matrix for Improving Bioavailability of Hydrophobic Drugs

In pharmaceutical industry, hydrophobic therapeutic drugs are often required to be mixed with water-soluble materials with the intention of adjustment of the drug potency and increasing the bioavailability of the drugs. A number of attempts have been made to improve the poor water solubility of hydrophobic drugs, as reviewed later (Section 1.5). One of the well investigated methodologies for improving the aqueous solubility a drug involves the use of an amorphous solid dispersion (ASD) (Taylor & Zografi, 1997; Leuner

& Dressman, 2000; Chadha et al., 2006; Ilevbare et al., 2013; Huang & Dai, 2014). In the ASD technique, hydrophobic drug molecules are dispersed at the molecular level in noncrystalline phase of a water-soluble matrix (Leuner & Dressman, 2000; Ilevbare et al., 2013; Huang & Dai, 2014; Newman et al., 2012; Li et al., 2013). A molecular-level mixture of a hydrophobic drug and water-soluble carrier substance can be obtained by hot melt extrusion (Sarode et al., 2013; Agrawal et al., 2016). Drying in the presence of an amphiphilic polymer(s) as a drug carrier material also has been known to be effective for the dispersion of highly hydrophobic drugs in a solid (Newman et al., 2012; Liu et al., 2015; Baghel et al., 2016). Furthermore, the use of a combination of a surface active agent with an amphiphilic polymer has been reported to further improve the ASD technique (Jie et al., 2009; Chaudhari & Dugar, 2017).

Here, the sugar amorphization technique based on the over-dissolution of sugar in alcohol (Section 1.2.) can be applied to the ASD of hydrophobic drugs (Sole-Amorphous-Sugar-based Solid Dispersion, SAS-SD) (Fig. 1.2.1). Namely, when an amorphized sugar preparation is dissolved in an organic solvent such as methanol, together with a hydrophobic drug, the hydrophobic drug is expected to be dispersed in the resulting dried amorphous sugar at a molecular level (Fig. 1.2.1).

In order to compare the SAS-SD technique with the others, the existing techniques and challenges to improve the solubility of hydrophobic drugs in water are reviewed in Section 1.6.

1.4. Purpose of this Study

This study aimed the following two:

1) Application of the alcohol-originated amorphous sugar matrix to the ASD of hydrophobic drugs
2) Physicochemical properties of alcohol-originated amorphous sugar

In Chapter 2, SAS-SD samples, in which hydrophobic model drugs were embedded, were prepared, utilizing the over-dissolution of sugar in alcohol. Four BCS Class II drugs and four sugars were used as representative fat-soluble model drugs and a water-soluble matrix, respectively. The sugar/drug mixture dissolved in methanol was vacuum foam dried. The SAS-SDs permitted drugs to be dissolved at 20%~1,000% higher than their

normal solubility at the initial stage of the dissolution in water when α-maltose or palatinose were used as sugars. These findings demonstrate the feasibility of using this novel solid dispersion technique for improving the water-solubility of water-insoluble (hydrophobic) drugs. However, the matrix of the solid dispersion, obtained from the organic solvent (methanol), showed a markedly (~50˚C) lower glass transition temperature than that from an aqueous solution.

In Chapter 3, the physicochemical properties of a sugar in the dried matrix and in organic solvents were focused on. α-Maltose and methanol as a representative sugar and organic solvent were used. Results suggest that the markedly low T_g for the methanol-originated amorphous sugar matrix is closely related to the compact conformation of □-maltose in an organic solvent. Secondly, a heat treatment was investigated for influencing the physical stability (T_g) of the SAS-SD and the aqueous dissolution of hydrophobic drugs from the surfactant-free solid dispersion. The heat treatment under appropriate conditions resulted in an increase in T_g of the methanol-originated solid dispersion. The dissolution of hydrophobic drugs (indomethacin and ibuprofen) in water from the surfactant-free solid dispersion was also improved as the result of the heat-treatment although, to the contrary, the dissolution of another model drug (curcumin) was lowered.

In Chapter 4, amorphous sugar (α-maltose, palatinose, trehalose) matrices were prepared from alcohol (methanol or ethanol) and their water sorption behavior and glass transition temperatures were compared with authentic samples that had been freeze-dried from water. Vacuum-foam- and spray-drying were employed as the drying methods. IR absorption spectra of the samples were also analyzed to evaluate the degree of hydrogen bond formation in the amorphous sugar samples. Finally, in summarizing the obtained findings, we discuss the impact of solvent type as well as the drying method on the physicochemical characteristics of an amorphous sugar matrix.

Finally, in Chapter 5, the whole thesis was discussed to give a conclusion. The perspectives of this study were also discussed.

1.5. Physicochemical Characteristics of (Authentic) Amorphous Sugars

1.5.1. Degree of Intermolecular Hydrogen Bond Formation

Amorphous sugar matrix is formed through the intermolecular hydrogen bonds, and the hydrogen bonding state of sugar molecules in the amorphous matrix is a substantial characteristics, possibly determinant for the other physicochemical characteristics. The IR absorption frequency of O–H stretching vibration of a sugar is essentially considered to represent the degree of formation of hydrogen bonds: The greater extent of intermolecular hydrogen bonds results in greater restriction of molecular vibrations and thus the lower frequency of O-H stretching vibration. The peak wavenumbers of IR band due to sugar O-H stretching vibration (at 25˚C), $\nu_{O\text{-}H}$, were retrieved from the reported/measured IR spectra and are listed in Fig. 1.5.1. As shown in Fig. 1.5.1, the OH wavenumber tends to be larger with increasing sugar molecular size. This suggests that larger sized sugar tends to form less hydrogen bondings in the amorphous sugar

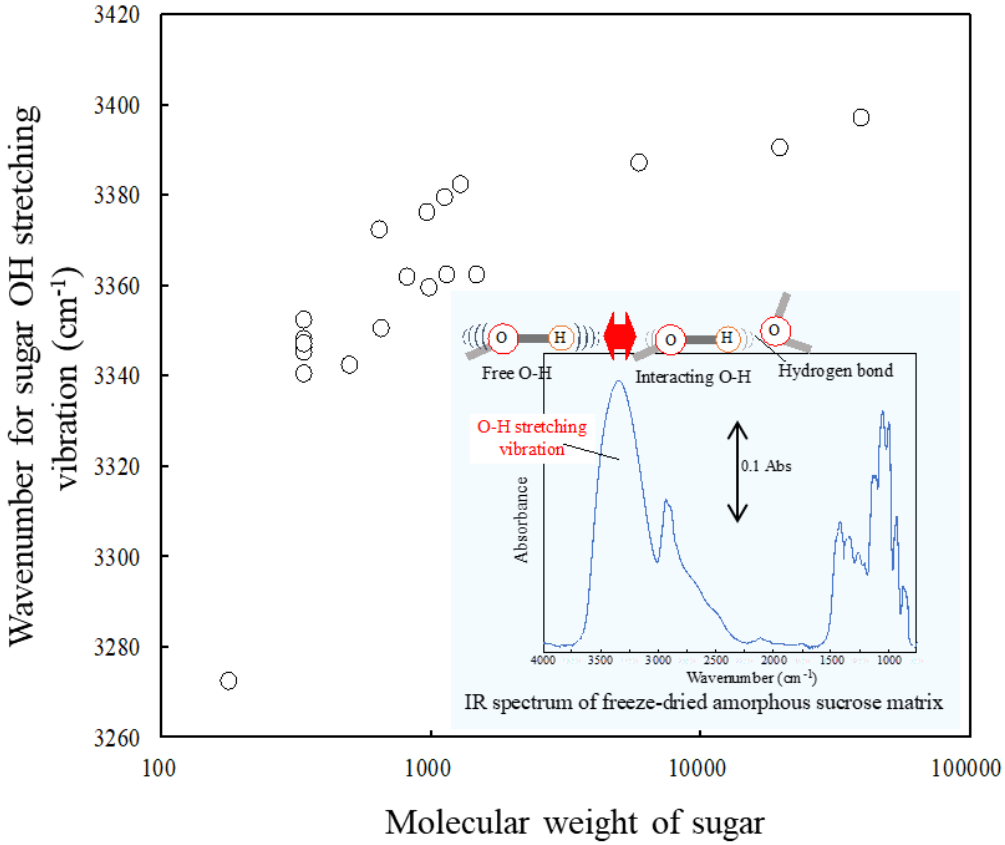

Fig. 1.5.1. Relationship between IR absorption frequency of sugar OH stretching vibration band and sugar molecular size

matrix. Such a tendency is typical for carbohydrates (Wolkers et al., 2004; van den Dries et al., 2000), and was indicated to happen because larger pyranose oligomers form a less densely packed matrix (Wolkers et al., 2004).

1.5.2. Water Sorption Behavior

A typical amorphous sugar matrix is hygroscopic and takes up water vapor onto and into the matrix. Sorbed water plays important roles in the physical properties of an amorphous sugar matrix (Slade & Levine, 1991; Roos & Karel, 1991a). Water sorption isotherms for freeze-dried amorphous matrices, comprised of representative types of sugars, are shown in Fig. 1.5.2 (Imamura et al., 2010a). The water content in the monolayer, W_m (g-water/g-dry matter), were determined by the approximation of the

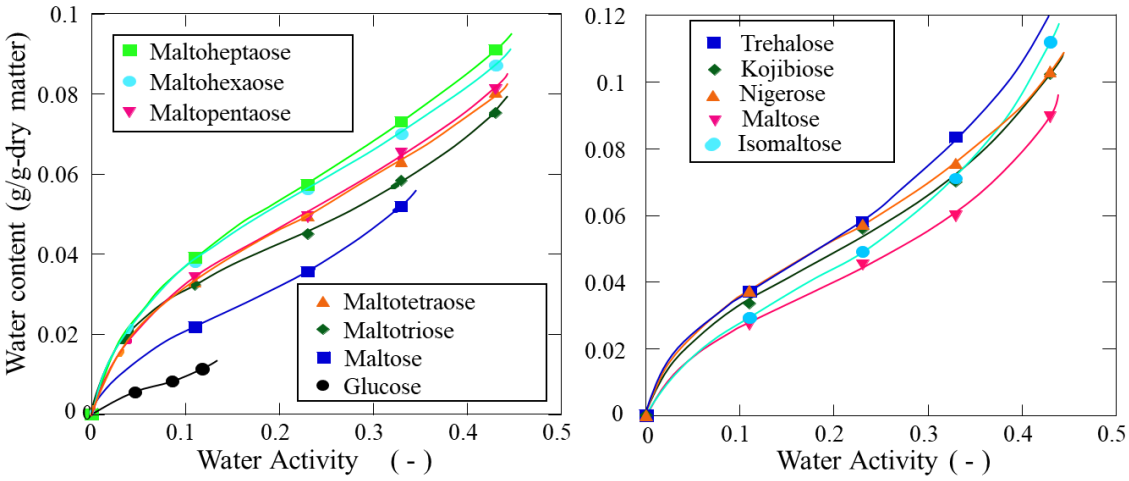

Fig. 1.5.2. Water sorption isotherms of (a) freeze-dried linear malto-oligosaccharides and (b) disaccharides (25°C) (Imamura et al., 2010)

sorption isotherm with a GAB equation (van den Berg & Bruin, 1981), are plotted against corresponding $\nu_{O\text{-}H}$ values in Fig. 1.5.3. The relationship between W_m and $\nu_{O\text{-}H}$ values for different types of linear oligosaccharides can be represented by a single curve. This may mean that

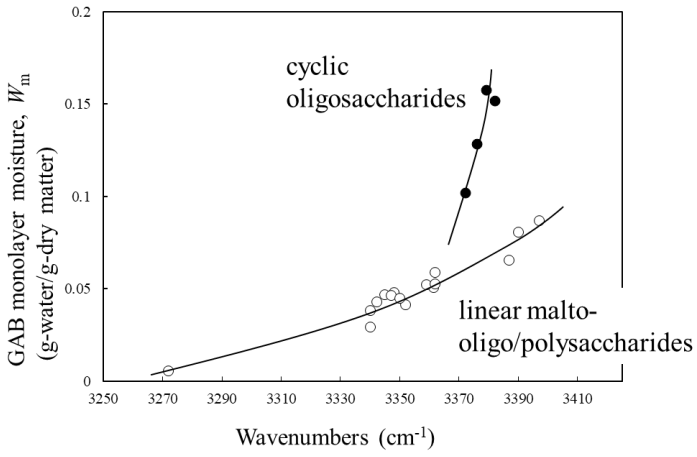

Fig. 1.5.3. Relationship between GAB monolayer moisture, W_m, and IR band frequency for sugar OH stretching vibration

the free O-H groups in amorphous matrix serve as water sorption sites. On the other hand cyclic oligosaccharides exhibit greater increase in W_m with increasing $\nu_{O\text{-}H}$ value. This may relate to substantially lower flexibility of molecular structure of cyclic sugars than that of linear saccharides.

1.5.3. Glass Transition Temperature

The glass-to-rubber transition behavior, especially the glass transition temperature (T_g), of various amorphous sugar matrices have been investigated (Orford et al., 1990; Roos & Karel, 1991b; Slade & Levine, 1991), and relationships between the T_g of amorphous sugar to the molecular weight of the sugar (Orford et al., 1990; Roos & Karel, 1991b), moisture content (Roos & Karel, 1991a), type and content of additives (te Booy et al., 1992 ; Shamblin et al., 1996), and related issues (Imamura et al., 1998; Ohtake et al., 2004), have been reported. The T_g values for amorphous sugars (thoroughly dehydrated) are plotted against their molecular weights in Fig. 1.5.4. The T_g value becomes higher with molecular weight. On the other hand, amorphous trehalose shows a significantly higher T_g value (108˚C) than the other disaccharides. The T_g for sucrose is much lower

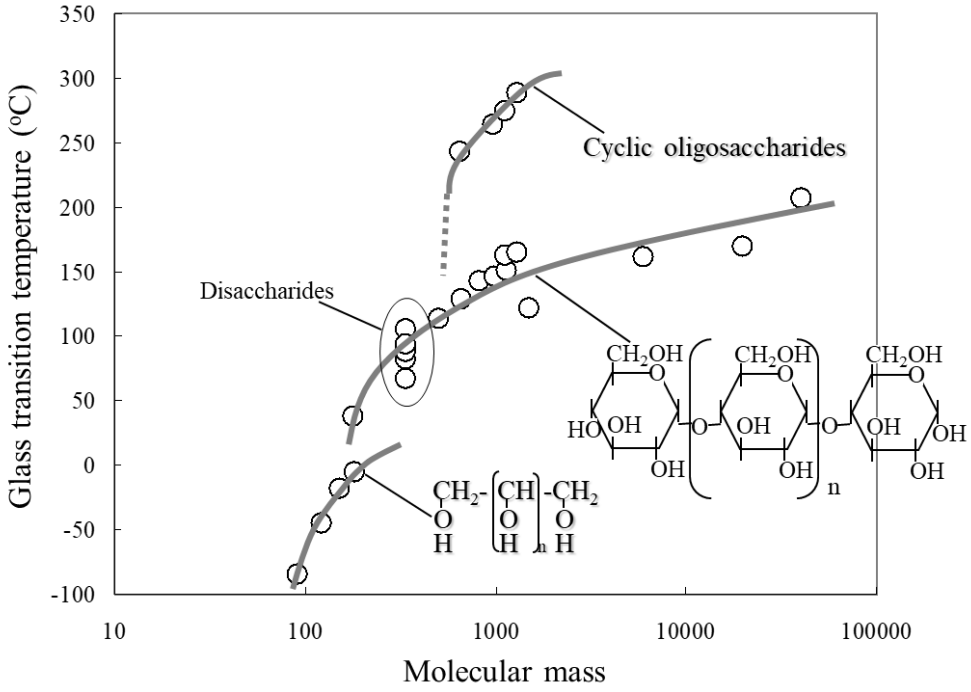

Fig. 1.5.4. Glass transition temperatures, T_g, for amorphous matrices of various sugars

than those for diglucoses although the T_g values for glucose and fructose are reported to be almost the same (Slade & Levine, 1991). It should be noted that the T_g value exhibits stepwise increase when the structure of sugar molecule turns from linear sugar alcohol to linear and then cyclic oligosaccharides. This may suggest the difference in glass-to-rubber transition among linear polyol, linear and cyclic oligosaccharides.

The T_g of an amorphous sugar matrix decreases with an increase in the amount of sorbed water (Roos & Karel, 1991a). To date, the relationship between T_g and amount of sorbed water has been measured for various types of sugar, and recently, the focus has been changed toward understanding the molecular mechanism responsible for lowering the T_g of amorphous sugar due to water sorption (Imamura et al., 2012; Kagotani et al., 2013).

1.5.4. True Density

The true density of amorphous sugar matrix is one of the physical properties, which describes the packing state of segment molecules in the matrix. It has been reported that the packing state of sugar molecules in the amorphous matrix is determinant for the mobility of matrix segments (sugar molecules) (van den Dries et al., 2000) and probably the formation characteristics of hydrogen bondings for a sugar, which have an impact to the glass-to-rubber transition behavior (van den Dries et al., 2000; Imamura et al., 2006). The impact of it may possibly reach water permeability, compactability, and stabilizing effect on the embedded molecules of an amorphous sugar matrix. To date, the densities of decent number of amorphous sugar matrices prepared by a spray drying were measured by a dry

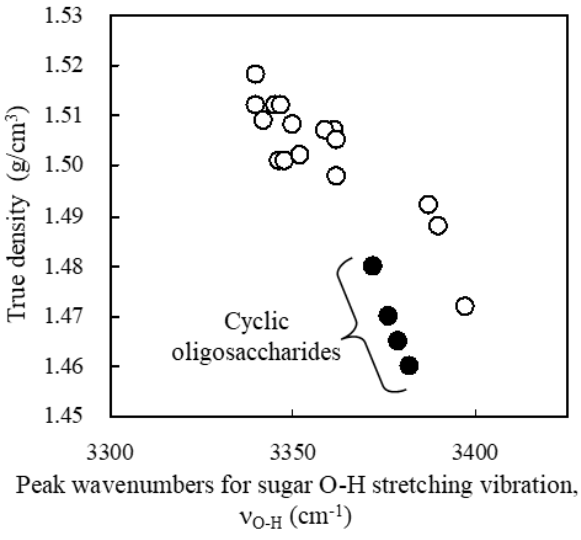

Fig. 1.5.5. Relationship between true densities for freeze-dried linear (open keys) and cyclic oligo-(/poly)saccharides (closed keys) and degree of intermolecular hydrogen bond formation, $\nu_{O\text{-}H}$ (Imamura et al., 2010)

gas pycnometric technique (Hancock & Zografi, 1994; Elversson & Millqvist-Fureby, 2005; Sun, 2005; Imamura et al., 2008). The true densities for freeze-dried samples of linear oligo-/polysaccharides and cyclic oligomers are shown as a function of $\nu_{O\text{-}H}$. Figure 1.5.5 shows a clear correlation between $\nu_{O\text{-}H}$ and true density value while the true density for cyclic oligosaccharide exhibits steeper decrease with increasing $\nu_{O\text{-}H}$. This means that more sugar-sugar hydrogen bonds are formed in more densely packed sugar matrix.

1.5.5. Crystallization Characteristics

Since the crystallization of amorphous sugar matrix results in the fatal loss of the functions, numerous studies have been reported on the crystallization behavior of an amorphous sugar matrix (Saleki-Gerhardt & Zografi, 1994; Kedward et al., 1998; Kedward et al., 2000a; Levenson & Hartel, 2005; Kawakami et al., 2006). The kinetics of crystallization have been investigated with respect to the effects of conditional variables, including temperature (Kedward et al., 1998; Kedward et al., 2000a), water sorption (Saleki-Gerhardt & Zografi, 1994; Kawakami et al., 2006; Kedward et al., 2000b; Harnkarnsujarit & Charoenrein, 2011) and related phenomena (Saleki-Gerhardt & Zografi, 1994; Kawakami et al., 2006; Bhugra et al., 2008). Many model equations for describing the crystallization of an amorphous sugar matrix have been proposed (Kedward et al., 1998; Kedward et al., 2000a; Kawakami et al., 2006). As a result, the crystallization of an amorphous sugar matrix has been known to generally require an induction period before the start of crystallization (Kedward et al., 1998; van Scoik & Carstensen, 1990). The induction period is

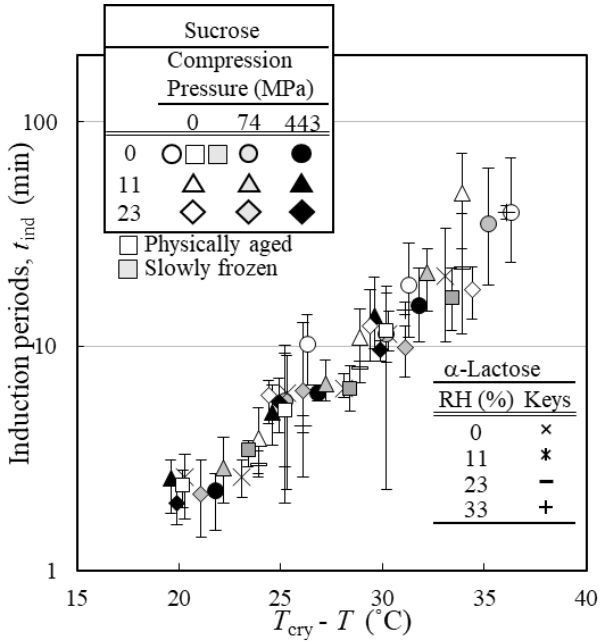

Fig. 1.5.6. Relationship between induction periods, t_{ind}, and crystallization temperature, T_{cry} T denotes the temperature used in the isothermal crystallization test. (Imamura et al., 2012)

an indicator of how long the amorphous state can be sustained under given conditions and is therefore essential for understanding and evaluating the stability of the amorphous state. The t_{ind} values for the different samples (sugar type, treatment, additive, etc) are shown in Fig. 1.5.6, where the horizontal axis means the difference between T_{cry} and temperature during the crystallization test, T (Imamura et al., 2012). The t_{ind} value is significantly decreased with increasing temperature and by water sorption, as generally expected (Kedward et al., 1998; Kedward et al., 2000b). Compression tends to cause a decrease in the t_{ind} value, as shown by Fig. 1.5.6, which has also been observed in thoroughly dehydrated systems (Kawakami et al., 2006; Imamura et al., 2010b). Slow freezing and physical aging also result in a shorter t_{ind}. It should be noted that plots of t_{ind} against ($T_{cry} - T$) appear to give a common curve, irrespective of the sugar type, treatment, and additive type. This suggests that the duration, within which an amorphous sugar matrix is maintained in an amorphous state, can be predicted from the value of T_{cry} and the storage temperature.

1.6. Techniques to Improve Water Solubility of Hydrophobic Drugs

Many chemicals which have therapeutic effects have been synthesized or discovered. However, many of the drug candidates are poor in aqueous solubility and thus bioavailability (Wadke et al., 1989; Lipinski, 2002; Thayer, 2010). Hence, huge number of challenges to improve the drug dissolution have been conducted, and the following techniques have been reported.

1.6.1. Prodrug

In the synthetic chemical approach, the prodrug method is the effective method to enhance the solubility of drugs (Stella, 2004; Stella, 2007; Rautio et al., 2008). In recent years, approximately 5-7% of commercialized drugs are prodrugs (Rautio et al., 2008; Stella, 2004). The prodrug method involves that drug molecules are preliminarily modified with hydrophilic moieties such as mannitol (Stella, 2010; Marinaro et al., 2012; Lopalco et al., 2021), and phosphonic groups (Sobue et al., 2004; Stella, 2007) to enhance the solubility; Modified drug molecules, namely prodrugs are metabolized through *in vivo* cleavage and return to their original drug molecules in the human body (Banerjee & Amidon, 1985; Stella et al., 1985).

1.6.2. Miniaturization of Drug Crystal Particle

As the crystal particle of drug is size-reduced, the surface area of drug crystal particle and thus the dissolution rate is increased (Kesisoglou et al., 2007). Milling (van Eerdenbrugh et al., 2008; Salazar et al., 2014; Shah et al., 2016), high-pressure homogenization (van Eerdenbrugh et al., 2008; Shah et al., 2016; Zhao et al., 2009), precipitation and recrystallization from suspension (Zhao et al., 2009; Sinha et al., 2013), and inducing crystallization of amorphous drugs embedded in polymer matrices by re-humidification or heating (Thombre et al., 2012) have been employed for the miniaturization.

1.6.3. Drug-Loaded-Porous Material

In recent years, there are various porous materials (adsorbent particles) that are commercially available. The porous materials that adsorb and release the hydrophobic drug molecules adequately, depending on the situation, can be used as a carrier for the hydrophobic drugs (Shivanand & Sprockel, 1998; Sher et al., 2007; Li et al., 2012). Namely, the porous carrier can hold considerable amount of hydrophobic drug on its large surface, and the drug molecules are stably delivered to the desired tissue. The drug-loaded carrier has been prepared by mixing the drug component with silicate (Ahuja & Pathak, 2009; Li et al., 2012; Nagane et al., 2014) and saccharide (Ahuja & Pathak, 2009; Saffari et al., 2016).

1.6.4. Drugs Entrapped in O/W Emulsion or between Lipid Bilayers

Since hydrophobic drugs usually are homogeneously dispersed in an oil phase, they can be stably entrapped in the O/W emulsion droplets. When the suspension of the drug-loaded oil droplets were dried into solid particles under appropriate conditions, the hydrophobic drug can be turned into a solid-state formulation (Porter et al., 1996). The emulsification-based technique has been reported as one of the effective techniques to enhance the drug solubility (Benita & Levy, 1993; Porter et al., 1996; Pouton, 1997).

Lipid bilayer in liposome also provides hydrophobic surroundings that can embed hydrophobic drug molecules. It has been reporeted that liposome stably holds hydrophobic drug molecules in the lipid bilayer and, in the administration, serves to improve the drug solubility in the aquous system (Chang & Yeh, 2012; Sriraman &

Torchilin, 2014; Torchilin, 2005).

1.6.5 Solid Dispersion

Amorphous materials, which can be regarded as a frozen solid, are one of the promising approaches to enhance the water solubility of hydrophobic drugs (Brouwers et al., 2009; Matteucci et al., 2009; Gao & Shi, 2012; Satoh et al., 2016). That is, when a hydrophobic drug is amorphized and then mixed with a poor solvent (=water), the drug molecules temporally are dispersed in the solvent and thus behave as dissolved molecules, resulting in the (temporal) increase in the drug solubility in water. This phenomenon is referred to as "super-saturation (Brouwers et al., 2009; Matteucci et al., 2009; Gao & Shi, 2012)" or "over-dissolution(Satoh et al., 2016)." However, since amorphous drugs are commonly likely to crystallize (Leuner & Dressman, 2000; Ilevbare et al., 2013, Li et al., 2013), they need to be combined (mixed) with a substance (carrier former) that can preclude the drug crystallization. Consequently, the amorphization of hydrophobic drugs in the presence of carrier forming substance is recognized as "amorphous solid dispersion (ASD)" technique (Leuner & Dressman, 2000; Ilevbare et al., 2013, Li et al., 2013). Amphiphilic polymer (such as polyvinylpyrrolidone (PVP) (Taylor & Zografi, 1997; Li et al., 1999; Modi & Tayade, 2006; Ha et al., 2014; Meng et al., 2021), hydroxypropyl methylcellulose (HPMC) (Won et al., 2005; Kennedy et al., 2008; Nguyen et al., 2016; Yu et al., 2020), Soluplus® (Lust et al., 2013; Lavra, 2017; Prasad et al., 2017; Mukesh et al., 2021) Eudragit® (Ruby et al., 1995; Aceves et al., 2000; Qi et al., 2008; Fan et al., 2020) or the combination of a surfactant with carbohydrate are usually used as a carrier of solid dispersions for hydrophobic drugs (Lai et al., 2009, Yadav V. B. & Yadav A. V., 2009). In recent years, solid dispersions were prepared by various methods (drying solution of a carrier and a hydrophobic drug (Singh & van den Mooter, 2016; Ogawa et al., 2018), melting and quenching (Repka et al., 2012; Patil et al., 2016), granulation (Cho et al., 2010; Jang et al., 2014), co-precipitation (Sekikawa et al., 1978; Schenck et al., 2019), and enhanced the water solubility of hydrophobic drugs (Singh & van den Mooter, 2016; Ogawa et al., 2018; Repka et al., 2012; Patil et al., 2016; Cho et al., 2010; Jang et al., 2014; Sekikawa et al., 1978; Schenck et al., 2019).

Chapter 2 Sole-Amorphous-Sugar-based Solid Dispersions (SAS-SDs) of Hydrophobic Drugs in an Amorphous Sugar Matrix Dried from an Organic Solvent

2.1. Introduction

Novel chemicals that have the potential for producing great therapeutic effects are being produced every day. However, many of these new therapeutic agents are water-insoluble (Wadke et al., 1989; Lipinski, 2002; Thayer, 2010). The poor water solubility of therapeutic drugs is a serious drawback that lowers the bioavailability of the drug.

To date, many attempts have been made to improve the solubility of hydrophobic drugs in physiological fluids. Chemical modification to produce a water soluble product represents one such approach to solving this problem (Amidon, 1991). One of the physicochemical approaches is to reduce the size of insoluble drug crystals to the nano level in order to increase the available surface area and thus the dissolution rate (Amidon, 1991; Thombre et al., 2012; Shah et al., 2016). Combining porous (and inert) particles as a carrier for hydrophobic drugs also has been reported to improve the bioavailability of a drug (Shivanand &Sprockel, 1998; Sher et al., 2007; Li et al., 2013). Hydrophobic drug molecules can also be entrapped in O/W emulsion droplets (Benita & Levy, 1993; Porter et al., 1996; Pouton, 1997; Jayne & Rees, 2000) or between lipid bilayers (Torchilin, 2005) for being administered to the human body in the dissolved state.

An alternate methodology for improving the water solubility of a hydrophobic drug is based on the amorphization of the drug (Hancock & Parks, 2000). Namely, the amorphous state can be regarded as a frozen solid of the constituents in the amorphous material, and when the constituent molecules are dispersed in a solvent in which the constituents are poorly soluble, it follows that they would temporarily behave as dissolved materials, a phenomenon that is referred to as “super-saturation (Brouwers et al., 2009; Matteucci et al., 2009; Gao & Shi, 2012)” or “over-dissolution (Satoh et al., 2016).” It has actually been demonstrated that the water solubility of a water-insoluble drug can be approximately doubled as the result of amorphization (Hancock & parks, 2000; Lloyd et al., 1997; Taylor & Zografi, 1997; Pokharkar et al., 2006). Since amorphous hydrophobic drugs are usually unstable and have a tendency to crystallize, they are often amorphized in the presence of carrier matrix forming agents (Leuner & Dressman, 2000; Ilevbare et al., 2013; Li et al., 2013). This strategy is categorized as a solid dispersion

(Leuner & Dressman, 2000; Ilevbare et al., 2013; Li et al., 2013). In the solid dispersion of water-insoluble drugs, an amphiphilic polymer such as polyvinylpyrrolidone is frequently used as the carrier matrix (Chadha et al., 2006; Huang & Dai, 2014), and a combination of a surfactant with an amorphous carbohydrate matrix has also been reported to be effective for the stable dispersion of drugs (Jie et al., 2009, Yadav B. V. & Yadav A. V., 2009).

On the other hand, "over-dissolution" can also occur in a system that is composed of a water-soluble solute and a fat-soluble solvent, which permits the preparation of a Sole-Amorphous-Sugar-based Solid Dispersion (SAS-SD) of fat-soluble oily substances in a dried amorphous sugar matrix (Satoh et al., 2016; Flores et al., 2002) as follows: (i) The sugar is amorphized and (ii) added to an organic solvent containing a hydrophobic substance, followed by homogenization. (iii) The homogenized solution is then dried to a solid (SAS-SD) under appropriate conditions. Our previous study revealed that an oily volatile flavor such as cinnamaldehyde can be stably embedded in a SAS-SD without any evidence of sugar crystallization or segregation of the oily flavor (Satoh et al., 2016; Patent No. 6524744). All of these findings suggest that the application of the SAS-SD technique for preparing an amorphous mixture of a hydrophobic drug and a sugar and to further enhance the water solubility of a hydrophobic drug is a feasible approach to the problem. The development of a SAS-SD technique would also contribute to expanding the types of carrier matrix materials that would be available for hydrophobic drugs.

In this study, SAS-SDs, with hydrophobic model drugs embedded in them, were prepared, using the above described procedures. Four BCS Class II drugs (Kasim et al., 2004) and four sugars were used as model fat-soluble drugs and water-soluble matrices, respectively. The sugar/drug mixture, dissolved in methanol, was vacuum foam dried (Walters et al., 2014). Characteristics of the resulting SAS-SD, including glass transition temperature, crystallinity, microscopic texture, and elemental distribution, were then examined. Changes in the water solubility of hydrophobic drugs due to their being dispersed in an amorphous sugar matrix were investigated by comparing the profiles for the release of the drug into water from the SAS-SD and crystalline samples of the drug.

2.2. Materials and Methods

2.2.1. Materials

Trehalose, maltitol, α-maltose, and palatinose were obtained from Wako Pure Chemical Industries, Ltd. (Osaka, Japan). Indomethacin (γ-form of the crystal) (Amidon et al., 1995), ibuprofen (Kasim et al., 2004), gliclazide (Amidon et al., 1995; Löbenberg & Amidon, 2000), nifedipine (Sutton et al., 2006) (Wako Pure Chemical Industries) (Fig. 2.2.1) were used as BCS Class II hydrophobic drugs. Polyvinylpyrrolidone (PVP, mean MW ~40,000) was the product of Nacalai Tesque (Kyoto, Japan). All of these chemicals were of reagent grade and were used without further purification.

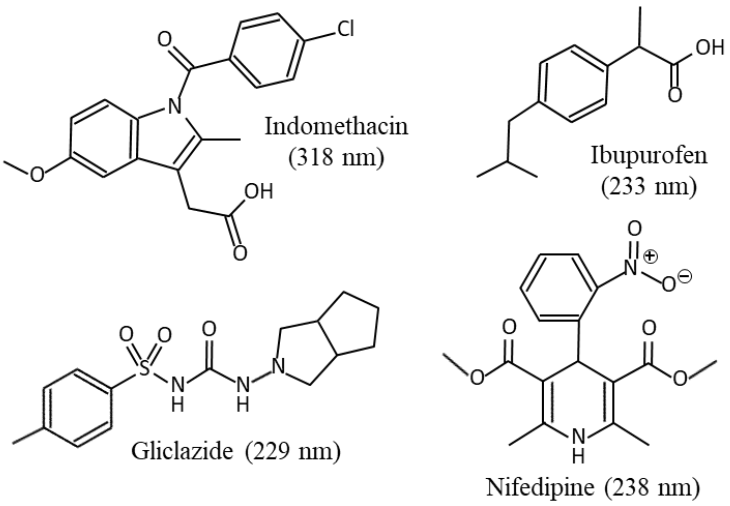

Fig. 2.2.1. The hydrophobic drugs tested in this study. Values in parentheses denote the specific UV absorption wavenumbers employed for the dissolved concentration measurements.

2.2.2. Preparation of SAS-SDs

An aqueous sugar solution was freeze-dried using the same procedure as was used in our previous study (Imamura et al., 2008). In a typical run, five milliliters of a solution containing 100 mg/mL of sugar was instantly frozen in liquid nitrogen and then freeze-dried at room temperature using a freeze-dryer (UT-80, EYELA TOKYO RIKAKIKAI Co., Tokyo, Japan) connected to a vacuum pump (GLD-100, ULVAC Japan, Ltd., Tokyo, Japan). The freeze-dried amorphous sugars were further dehydrated by storing them over P_2O_5 in a vacuum desiccator at 37˚C for more than three days. The content of remaining water after the dehydration was preliminarily measured by Karl-Fischer

coulometric moisture titration (Imamura et al., 2001) and confirmed to be less than the detection limit (0.002 g/g-dry sugar). The thoroughly dehydrated amorphous sugar cake was added to a methanol solution of a model hydrophobic drug. A 100 mg sample of the amorphous sugar was typically added to 1 mL of methanol in which 1 or 10 mg of the model drug had been dissolved. Alternatively, PVP was dissolved at a concentration of 100 mg/mL in the methanol solution, as an amphiphilic polymer for use in the existing solid dispersion technique (Chadha et al., 2006; Huang & Dai, 2014), instead of an amorphous sugar. Immediately thereafter, a 100 μL aliquot of the mixture solution was transferred to a 1.5 mL-polypropylene tube and the resulting solution was then dried under a reduced pressure of around ca. 1 Torr and centrifugation at 25±1˚C for 60 min (for α-maltose, palatinose, and maltitol) or 120 min (for trehalose), using a TOMY Micro Vac MV-100 centrifugal concentrator (TOMY SEIKO Co., ltd., Tokyo, Japan). At this initial drying stage, foaming was minimal. After the initial drying, the residue was punctured with a steel needle, followed by the secondary vacuum drying for an additional 30 min. The subsequent vacuum drying immediately resulted in foaming 100% of the time. Alternatively, after different periods of vacuum foam drying, ten sampling tubes containing the sample solutions were weighed on analytical balance, from which the time course for the sample solution during the vacuum foam drying was determined.

Thermal drying techniques such as spray drying (Leuner & Dressman, 2000; Li et al., 2013) are frequently used for preparing solid dispersions. On the other hand, vacuum foam drying does not require heating and a high degree of dryness and be attained (Satoh et al., 2016), which is generally preferable for drying a combustible organic solvent. Accordingly, the vacuum foam drying described above was used.

The preliminary step of this study revealed that a 10%w/w drug loading for the SAS-SD sample caused a significant collapse during vacuum foam drying in the case of maltitol, while a 1%w/w drug loading did not induce any significant collapsing for all of the tested sugars. Hence, in this study, a drug loading of 1%w/w was assumed as the default. However, SAS-SDs containing 10%w/w model drug were also prepared in order to detect possible segregation, including crystallization of the model drug and phase separation into the sugar- and the drug-rich phases, by differential scanning calorimetry and energy dispersive X-ray spectroscopy, as described below.

2.2.3. Dissolution Behavior of Hydrophobic Drugs from Solid Dispersion Samples.

The prepared SAS-SDs of model hydrophobic drugs were added to a known amount of water (0.2~2 mL) and the suspension was stirred at 200 rpm with a 1.5-cm magnetic stirring bar at 37±1˚C throughout the dissolution experiment. A 200~1,000 μL aliquot of the suspension was withdrawn and then filtered with 0.2 μm pore size filter (Nihon Millipore K.K., Tokyo, Japan). The concentration of the dissolved model drug was typically measured by UV-vis absorption at specific wavelengths (Fig. 2.2.1), where the UV absorption of the drug was not overlapped with that of the sugar. In the dissolution tests for PVP-based solid dispersions of ibuprofen, gliclazide and nifedipine, the UV absorption due to the dissolved drug was determined at 263.5 nm for ibuprofen, 268 nm for gliclazide, and 353 nm for nifedipine, so as to avoid overlap with the UV-vis absorption shoulder of the PVP. The prepared SAS-SDs of model hydrophobic drugs were added to a known amount of water (0.2~2 mL) and the suspension was stirred at 200 rpm with a 1.5-cm magnetic stirring bar at 37±1˚C throughout the dissolution experiment. A 200~1,000 μL aliquot of the suspension was withdrawn and then filtered with 0.2 μm pore size filter (Nihon Millipore K.K., Tokyo, Japan). The concentration of the dissolved model drug was typically measured by UV-vis absorption at specific wavelengths (Fig. 2.2.1), where the UV absorption of the drug was not overlapped with that of the sugar. In the dissolution tests for PVP-based SAS-SDs of ibuprofen, gliclazide and nifedipine, the UV absorption due to the dissolved drug was determined at 263.5 nm for ibuprofen, 268 nm for gliclazide, and 353 nm for nifedipine, so as to avoid overlap with the UV-vis absorption shoulder of the PVP.

2.2.4. Differential Scanning Calorimetry

Differential scanning calorimetry (DSC) analyses of the SAS-SD samples were also conducted, in which a TA Q2000 calorimeter (TA instruments Co., New Castle, DE) equipped with an RCS90 cooling system (TA instruments Co.) was used. A 2.5~10 mg sample was hermetically sealed in a 20 μl aluminum pan and then scanned at a rate of 3˚C/min between -20 and 200˚C, using an empty aluminum pan as a reference. Thermal events, including the glass-to-rubber transition of the amorphous phase and melting of the crystal phase were analyzed from the obtained DSC thermograms.

2.2.5. Powder X-ray Diffractometry

Alternatively, SAS-SD samples were sufficiently powdered by grinding. The resulting fine powders were placed on a sample holder of an X-ray diffractometer PANalytical X'PERT PRO MPD system in Bragg-Brentano geometry with Cu-Kα radiation (PANalytical B.V., Almelo, Holland). X-ray diffraction patterns of the SAS-SD samples were then obtained using an X-ray tube voltage of 45 kV and a current of 40 mA, in which 2Theta range, scan speed, and step size (resolution) for data collection were 5~50˚, 3˚/min, and 0.04˚, respectively.

2.2.6. Scanning Electron Microscopy and Energy Dispersive X-ray Spectroscopy

The SAS-SD samples were coated with a thin film (ca. 40 nm) by evaporating a platinum/palladium alloy using a Hitachi E-1030 ion sputter instrument (Hitachi High-Technologies Co., Tokyo, Japan). The resulting samples were observed using a KEYENCE VE9800 scanning electron microscope system (KEYENCE Co., Tokyo, Japan) at an accelerating voltage of 15 kV. In the case where indomethacin was used as a model drug, the elemental distributions of chloride and oxygen in the SAS-SD sample was determined with a KEYENCE VE9800 EDAX system integrated with the SEM observation system.

2.3. Results

2.3.1. Vacuum Foaming Drying Process

Figure 2.3.1 shows representative drying processes of the methanol solution of sugar and a drug (indomethacin) during the vacuum foam drying. The vacuum foam drying was accompanied by foaming, which markedly accelerated the evaporation of methanol (Fig. 2.3.1). Foaming was reliably induced at a 100% probability by the needle-puncturing the sample with a needle after vacuum drying for an appropriate period, as described in the experimental section, irrespective of the fact that the foaming occurred without this procedure for some, but not all samples (Fig. 2.3.1). This needle stimulation-based technique to control the timing of foaming allowed the sample preparation to be reproducibly.

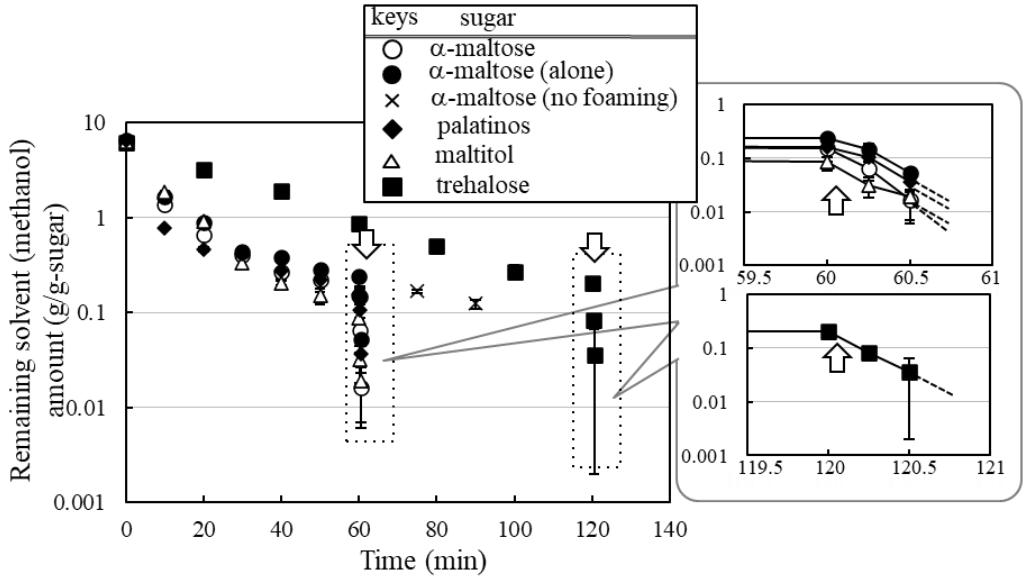

Fig. 2.3.1. Drying processes for methanol solutions containing sugar and a model drug (indomethacin) during vacuum drying at 25˚C. Initial concentrations of sugar and indomethacin were 100 mg/mL and 1 mg/mL, respectively, which corresponds to a 1%w/w indomethacin content in the solid dispersion. The solution volume was 100 µL. The drying process of the methanol solution containing only α-maltose is also shown. The arrow in the graph denotes the time point at which the vacuum drying was interrupted and the sample solution was then stimulated with a stainless steel needle, which resulted in the immediate foaming of the solution after the restart of the vacuum drying. The results for the absence of needle-stimulation are shown as cross marks.

As shown in Fig. 2.3.1, the drying process for the methanol solution of a sugar was essentially unchanged regardless of the presence or absence of 1%w/w indomethacin. In addition, there was no significant difference between the drying processes for the tested

sugars, except for trehalose (Fig. 2.3.1). On the other hand, it was found that a methanol solution containing trehalose was much more difficult to dry under a vacuum than those for the other tested sugars and required a much longer period of initial drying before needle puncturing to induce a 100% probability of foaming, compared to the other tested sugars. Hence, in the case of trehalose, the needle puncturing procedure was conducted after a 120 min-initial drying period whereas the methanol solutions for the other sugars were punctured after a 60 min-initial drying period. Consequently, the methanol solution containing trehalose exhibited a quite different drying process from those for the other sugars, as shown in Fig. 2.3.1.

2.3.2. Characterization of SAS-SD

Our previous study (Satoh et al., 2016) revealed that amorphous α-maltose was extremely soluble in methanol and could be stably mixed with fat-soluble substances. Accordingly, α-maltose is considered to be a quite suitable sugar for use in preparing a SAS-SD. On the other hand, the indomethacin molecule contains a chloride atom that can be analyzed to detect the distribution in the SAS-SD sample by energy dispersive X-ray spectroscopic analysis (EDX). Hence, a combination of α-maltose and indomethacin was employed as a representative preparation in the physicochemical analyses of the SAS-SDs.

Figure 2.3.2 shows the DSC thermograms of a pure drug (indomethacin) sample, that had been completely dissolved in methanol and then dried as well as the model drug in crystalline form. All of the pure drug samples showed strong endothermic peaks due to the melting of their crystals, as shown in Fig. 2.3.2. The DSC thermograms of the SAS-SDs of 1%w/w model hydrophobic drug (indomethacin) are also shown in Fig. 2.3.2 The SAS-SDs of model drugs showed no significant endothermic peaks. This indicates that both the sugar and model drug remained amorphous throughout the vacuum foam drying process. The fully amorphous nature of a SAS-SD of 1% model drug was also confirmed by power X-ray diffractometry analyses (Fig. 2.3.3).

As shown in Fig. 2.3.2, the SAS-SD sample containing 10%w/w indomethacin showed a faint endothermic peak at ca. 150˚C, which is ca. 10˚C lower than the melting point of the γ-form of indomethacin (Lin, 1992). This suggests that a trace of the α-form of crystalline indomethacin (Lin, 1992) was formed during the preparation of the SAS-SD

of 10%w/w indomethacin. However, the powder X-ray diffractometry did not detects any peaks for α-form of indomethacin (Fig. 2.3.3).

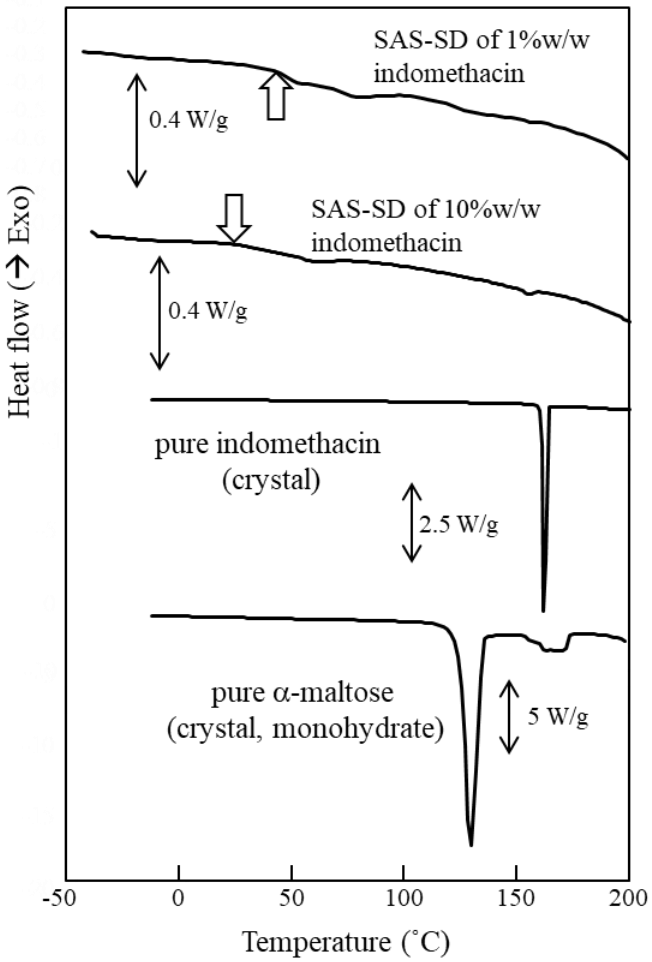

Fig. 2.3.2. DSC thermograms for Sole-Amorphous-Sugar-based Solid Dispersions (SAS-SDs) of indomethacin as well as their constituents (indomethacin and α-maltose). Solid dispersions were obtained from methanol solutions, containing 100 mg/mL α-maltose and 1 or 10 mg/mL indomethacin. Arrows in the graph denote T_g values.

Table 2.3.1. Glass Transition Temperatures (T_g) for SAS-SDs of Indomethacin as well as for Freeze-Dried Amorphous Matrices of Sugar Alone.

sugar	model drug	drug content (wt%)	T_g (˚C)
α-maltose	Indomethacin	0	36±1 (90±1)
		1.0	39±1
		10	21±1
	Ibuprofen	1.0	36±5
		10	22±4
	Gliclazide	1.0	30±1
		10	16±2
	Nifedipine	1.0	36±1
		10	32±1
palatinose	Indomethacin	0	21±1 (62±2)
		1.0	23±3
trehalose	Indomethacin	0	37±3 (102±3)
		1.0	37±4
maltitol	Indomethacin	0	9±2 (46±2)
		1.0	10±2

The values in parentheses are the T_g for amorphous matrix of sugar alone, freeze-dried from an aqueous solution.

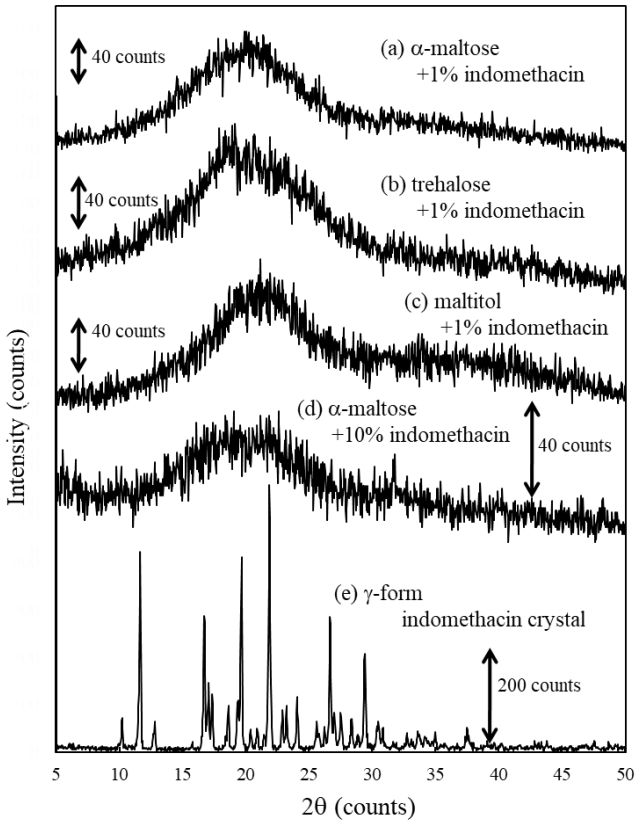

Fig. 2.3.3. X-ray diffraction patterns of (a-d) SAS-SDs of indomethacin and (e) γ-form indomethacin crystal

The SAS-SD samples showed a shift in the apparent heat capacity, which is assigned to a glass-to-rubber transition (Fig. 2.3.2). Table 2.3.1 lists the glass transition temperatures (T_g) for the SAS-SDs as well as those of amorphous matrices that are comprised solely of sugars. As shown in Table 2.3.1, the T_g values for the SAS-SD samples are, at most, slightly above room temperature, which could possibly allow the crystallization of sugar and/or drug molecules. A glassy structure with such a low strength in SAS-SD is a drawback of this novel solid dispersion technique.

Several classes of substances, including phosphate (Ohtake et al., 2004; Imamura et al., 2010a) and carboxylic compounds (Imamura et al., 2010a), serve to increase the T_g value of amorphous sugar matrices. On the other hand, it has been reported that polyacrylic acid forms a complex with basic drug compounds (Weuts et al., 2005), and hypromellose phthalate was also indicated to interact with a hydrophobic drug, clofazimine (Nie et al., 2015; Nie et al., 2016). Such interactions with hydrophobic drugs are expected to inhibit the crystallization of the drugs in the solid dispersions. Considering these, the addition of the T_g-increasing substance and/or the interaction counterpart of a drug may possibly

be effective for improving the storage stability of the SAS-SD.

Fig. 2.3.4(a) shows SEM images of an α-maltose-based solid dispersion of 10%w/w indomethacin. The rupture of a dried bubble shell resulted in the creation of small fractures in the dried sugar/drug mixture, as shown in Fig. 2.3.4(a). EDX elemental (oxygen and chloride atoms) mapping images for SAS-SD samples of indomethacin are shown in Fig. 2.3.4(b) and (c). No evidence of the localization of Cl atoms of the model drug (indomethacin) was observed in the SAS-SD sample, as shown in Fig. 2.3.4(c). This suggests that the model drug and sugar molecules were homogeneously mixed, possibly at the molecular level.

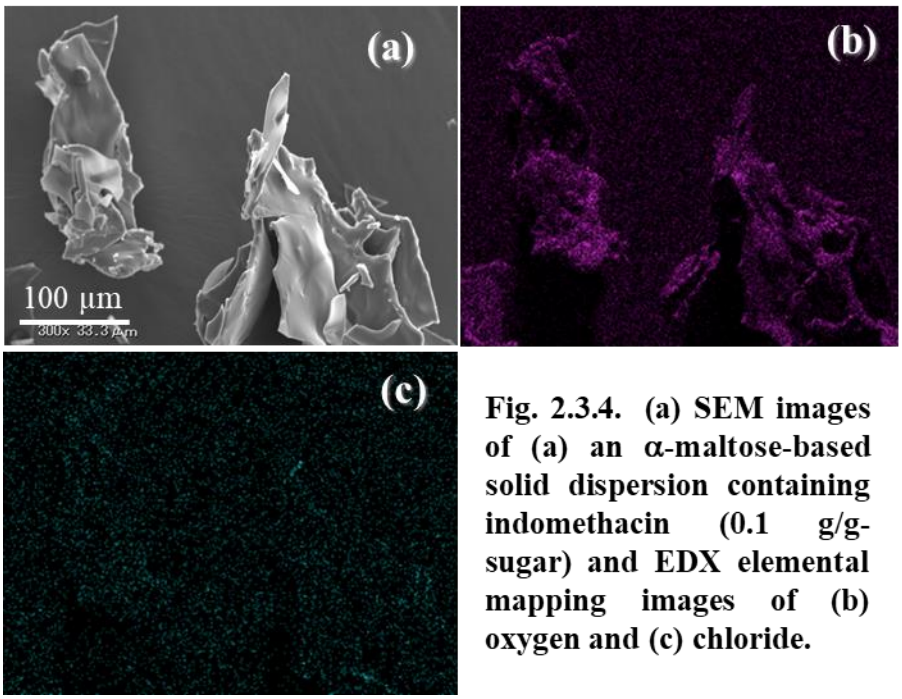

Fig. 2.3.4. (a) SEM images of (a) an α-maltose-based solid dispersion containing indomethacin (0.1 g/g-sugar) and EDX elemental mapping images of (b) oxygen and (c) chloride.

2.3.3. Dissolution Behavior of Hydrophobic Drugs from a SAS-SD

Fig. 2.3.5 shows the time courses for the concentration of model drugs from the SAS-SD samples containing different sugars as a carrier matrix. Except for nifedipine, the SAS-SD samples exhibited a typical "spring and parachute (Brouwers et al., 2009)" shape dissolution curve (Fig. 2.3.5): The concentration of the dissolved drug first increases above its solubility and then decreased to an equilibrium level equal to its solubility. Nifedipine also showed an increase in water solubility as the result of the SAS-SD, although no decrease in the dissolved concentration was observed within the tested time range, as reported in the literature (Suzuki & Sunada, 1998; Morteza et al., 2016). These

findings demonstrate that, although temporary, the SAS-SD technique can increase the solubility of a water-insoluble drug.

From the drug dissolution profiles shown in Fig. 2.3.5, the kinetic parameters, namely, the maximum concentration of dissolved drug [C_{max} (μg/mL)], the elapsed time for C_{max} [t_{max} (min)], the half-life of over-dissolution [$t_{1/2}$ (min)], and the area under the drug concentration-time curve [$AUC_{0\text{-}60min}$ (μg•min/mL)], were determined and the results are listed in Table 2.3.2. As indicated by the C_{max} values (Table 2.3.2), all of the drugs tested underwent over-dissolution, when α-maltose or palatinose is used to form a carrier matrix. However, the order for the increase in C_{max} and $AUC_{0\text{-}60min}$ for palatinose and α-maltose appears to vary, depending on the type of drug being tested. This demonstrates that a combination of a sugar and a drug may affect the dissolution behavior the drug.

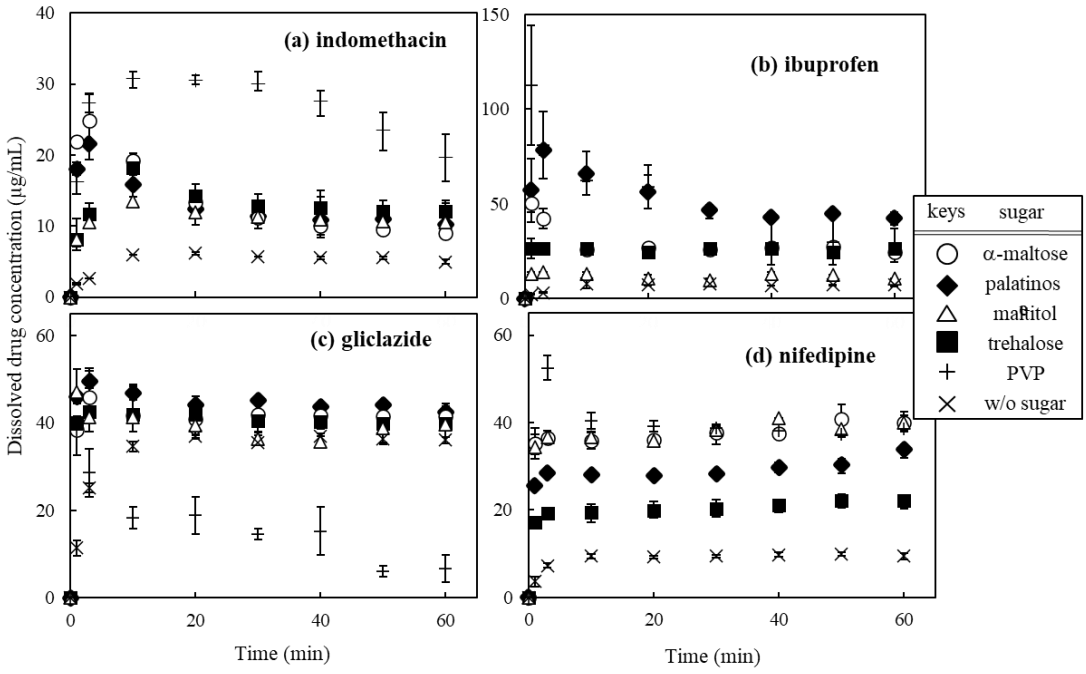

Fig. 2.3.5. Dissolution profiles of model drugs in water from a SAS-SD, containing different types of sugars and PVP. The drug content in the solid dispersion sample was 1%w/w. The amounts of model drug added to the water were 50 μg/mL for (a) indomethacin, 500 μg/mL for (b) ibuprofen, and 100 μg/mL for (c) gliclazide and (d) nifedipine.

Table 2.3.2. Kinetic Parameters Determined from the Drug Dissolution Profiles Shown in Fig. 2.3.5, namely, Maximum Concentration of Dissolved Drug [C_{max} (μg/mL)], Elapsed Time for C_{max} [t_{max} (min)], Half-Life of the Over-Dissolution [$t_{1/2}$ (min)], and Area under Drug Concentration-Time Curve up to 60 min [$AUC_{0\text{-}60min}$ (μg•min/mL)].

model drug	sugar	C_{max} (μg/mL)	t_{max} (min)	$t_{1/2}$ (min)	$AUC_{0\text{-}60min}$ (μg•min/mL)
indomethacin	α-maltose	24.8	~3	18	793
	trehalose	18.2	~10	35	797
	maltitol	13.5	~10	18	675
	palatinose	21.6	~3	19	767
	PVP	30.8	~10	>60	1623
	crystal	6	~10	-*	319
ibuprofen	α-maltose	50.5	~1	7	1683
	trehalose	27	~15	-*	1536
	maltitol	14.1	~3	15	706
	palatinose	81	~3	12	3121
	PVP	112.7	~1	8	2842
	crystal	7.4	~30	-*	404
gliclazide	α-maltose	46	~3	7	2489
	trehalose	42.5	~7	~25	2435
	maltitol	41.4	~7	~25	2310
	palatinose	49.6	~3	~15	2677
	PVP	38.4	~1	9	924
	crystal	37	~20	-*	2062
nifedipine	α-maltose	38.5	>40	-*	2242
	trehalose	22.2	>60	-*	1223
	maltitol	38.5	>40	-*	2264
	palatinose	33.9	>60	-*	1738
	PVP	52.5	~3	-*	2332
	crystal	9.8	~10	-*	548

* $t_{1/2}$ could not be determined since the dissolution profile did not involve the overshoot of the dissolved drug concentration.

Compared to the cases for α-maltose and palatinose, the C_{max} of a trehalose-based solid dispersion is usually markedly limited (Table 2.3.2). This may be related to the slower dissolution rate from the trehalose-based solid dispersion, as indicated by greater t_{max} relative to the α-maltose and palatinose samples (Table 2.3.2). Maltitol is also inferior in C_{max} and $AUC_{0\text{-}60min}$ to α-maltose and palatinose in the cases except for nifedipine, while the maltitol-based solid dispersion exhibited a comparatively large $AUC_{0\text{-}60min}$ in the case for nifedipine (Table 2.3.2).

The drug dissolution profiles from a PVP matrix were also measured (Figs. 2.3.5). As shown in Fig. 2.3.5(a), the PVP-based solid dispersion of indomethacin exhibits greater C_{max} and $AUC_{0\text{-}60min}$ than the other sugar-based compounds (Table 2.3.2). The $t_{1/2}$ for the PVP-based solid dispersion was also markedly greater than that for the other sugar-based ones (Table 2.3.2), indicating much slower decrease (parachute) of the dissolved concentration. However, as shown in Table 2.3.2, the C_{max} and $AUC_{0\text{-}60min}$ values for the SAS-SD of ibuprofen and nifedipine are in the same range as the PVP-based solid dispersion when an appropriate type of sugar is used. Furthermore, in the case for gliclazide, the presence of PVP caused significant precipitation in the dissolution test, resulting in a considerably small value for $AUC_{0\text{-}60min}$ (Table 2.3.2). Gliclazide was also observed to have a low solubility in the presence of PVP, when the crystalline preparation was dissolved in the presence of PVP. Considering these findings, the SAS-SD technique employed herein is expected to have the potential for serving as an alternative methodology for improving the bioavailability of water-insoluble drugs, although further investigation will, of course, be needed to understand the details of the process.

2.4. Discussion

Vacuum foam drying was investigated as an alternate technique for drying vaccines and biologics without any significant quality loss (Pisal et al., 2006; Walters et al., 2014). As demonstrated by Fig. 2.3.1, the drying process during the vacuum foam drying is strongly altered, depending on when foaming occurs. An extremely high vacuum in the drying chamber can cause foaming immediately after the start of the vacuum drying. However, in principle, the forming occurs probabilistically; In the case when a sufficient airtightness and exhaust velocity are unavailable, as in ordinary vacuum drying setups,

the timing of the foaming significantly varies, under most conditions. It follows that the drying processes and thus the dried product vary considerably, which is a significant drawback to the use of vacuum foam drying. On the other hand, in this study, it was eventually found that, when the vacuum drying was aborted after a certain period of drying and stimulated by puncturing the sample solution with a steel needle, this resulted in foaming to be initiated 100% of the time. The findings also indicate that the probability of foaming strongly depend on the extent of drying and the temperature at the time needle stimulation was conducted as well as the combination of solute and solvent being used. Further studies on the use of the needle stimulation-based technique to control the timing of foaming as well as the mechanism will be needed and should improve the applicability of the vacuum foam drying technique to the improvement of the bioavailability of a drug.

As shown in Table 2.3.1, the T_g value of the α-maltose-based solid dispersion of indomethacin decreased from ca. 40˚C to ca. 20˚C as the result of increasing the indomethacin content from 1%w/w to 10%w/w while the 1%w/w drug loading did not lower or slightly increase the T_g value. This indicates that the model hydrophobic drugs function to plasticize the amorphous sugar matrix (Satoh et al., 2016). It should be noted that amorphous matrices of sugars alone, when dried from a methanol solution, show T_g values that are several tens lower than the corresponding values from an aqueous solution. The solvent (methanol) molecules had been thoroughly removed from the SAS-SD sample, judging from the vacuum foam drying process (Fig. 2.3.1), and the T_g values for a sugar alone, prepared from an aqueous solution, are known to be independent of the drying method used (Surana et al., 2004). Accordingly, it must be concluded that the solvent (water or methanol) strongly affects the T_g value of an amorphous sugar matrix.

As shown in Fig. 2.3.4(a), the fractured flakes of an α-maltose-based solid dispersion sample were somewhat shrunken and rounded off relative to those of the solely foam-dried α-maltose (Satoh et al., 2016). This can occur when the decrease in T_g due to the presence of a comparatively large amount (10%w/w) of a hydrophobic substance (model drug) (Fig. 2.3.2 and Table 2.3.1) allows the dried matrix to partially collapse during the drying process.

When the highest C_{max} values for each model drug (Table 2.3.2) are compared, the overshoot for the dissolved drug concentration above its solubility are found to be in the

same order (40~90 nmol/mL [15~40 μg/mL on a mass concentration basis]), except for ibuprofen, while the water solubility of the drugs are markedly different (indomethacin, nifedipine: ~20 nmol/mL [~8 μg/mL]; gliclazide: 120 nmol/mL [~40 μg/mL]). This suggests that the extent of the over-dissolution of a hydrophobic drug may be determined mainly by the herein-employed SAS-SD technique as well as this dissolution condition, not by the original water solubility of the drug. On the other hand, the molecular size of ibuprofen is markedly smaller than the other three model drugs, which may allow more rapid diffusion into the bulk solution. Accordingly, the markedly low original solubility of indomethacin and nifedipine and the markedly small molecular size of ibuprofen are considered to result in a significant extent of over-dissolution (approximately four fold of C_{max} for indomethacin and nifedipine; approximately ten fold of C_{max} for ibuprofen) (Table 2.3.2). In contrast, due to the markedly high original solubility of gliclazide solubility, the over-dissolution of gliclazide from the SAS-SD presents a low profile (~20% greater C_{max} than its normal solubility) (Table 2.3.2).

2.5. Conclusions

Some model class II hydrophobic drugs including indomethacin, ibuprofen, gliclazide, and nifedipine were dispersed in an amorphous sugar matrix (SAS-SD) by the vacuum foam drying of methanol solutions containing a sugar and the model drug. SAS-SDs of indomethacin, and ibuprofen exhibited an extremely high over dissolution concentrations at the initial stage of the dissolution in water when α-maltose or palatinose was used as the sugar: The concentration of dissolved drugs temporarily increased up to 20%~1,000% of their water solubility. These findings demonstrate the feasibility of the novel SAS-SD technique for improving the water-solubility of water-insoluble drugs. Further investigations will be required to completely understand how the compatibility between a sugar and a drug affect drug dissolution behavior and expand the applicability of the SAS-SD technique to a wider variety of hydrophobic drugs.

Chapter 3 Physical Stability of an Amorphous Sugar Matrix Dried from Methanol as an Amorphous Solid Dispersion Carrier and the Influence of Heat Treatment

3.1. Introduction

An amorphous matrix composed of a sugar is a commonly used material in the drug industry. Various physicochemical aspects of amorphous sugar matrices including water sorption (Slade & Levine, 1988; Slade & Levine, 1991; Hancock & Shamblin, 1998), crystallization (Hartel & Shastry, 1991; Kedward et al., 1998; Saleki-Gerhardt & Zografi, 1994; Kedward et al., 2000b), encapsulation characteristics (Crowe et al., 1987; Jonsdottir et al., 2005; Desai & Park, 2005; Gharsallaoui et al., 2007), and stabilizing effect of labile proteins (Franks et al., 1991; Pilal, 1994; Carpenter et al., 1994), have been extensively investigated over the years in the fields of pharmaceutical technology and carbohydrate research. Glass-to-rubber transition behavior is one of the commercially important and thus well-investigated issues since it diminishes the functionalities of an amorphous sugar matrix (Chang et al., 1996; Bhandari et al., 2005; Carolina et al., 2007; Imamura et al., 2009).

The glass transition temperature, T_g, is frequently used to characterize the transitions between glassy and rubbery states of an amorphous sugar matrix. The T_g value and its dependence on different conditions have been analyzed for various types of sugars (Slade & Levine, 1988; Slade & Levine, 1991; Roos & Karel, 1990; Orford et al., 1990; Liu et al., 2006). It is generally accepted that a larger size sugar tends to form an amorphous matrix with a higher T_g value (Slade & Levine, 1988; Orford et al., 1990; Roos & Karel, 1991b) but the glycosidic linkage site also affects the T_g value (Imamura et al., 2006). The most influential factor may be the amount of water that is contained in the amorphous matrix (Slade & Levine, 1988; Tsourouflis et al., 1976). Water molecules that are sorbed in the amorphous sugar matrix function to plasticize the matrix and thus lower the T_g value (Roos & Karel, 1991b; Roos & Karel, 1991c) although the impact of the sorbed water on the T_g value is substantially different and is dependent on the interaction states of the water molecule (Imamura et al., 2012; Kagotani et al., 2013). A variety of substances have been extensively investigated and some have been found to significantly alter the T_g value of an amorphous sugar matrix (Orford et al., 1990; Taylor & Zografi, 1998; Miller et al., 1999; Imamura et al., 2010).

In contrast, it is generally thought that the method used to prepare an amorphous sugar matrix does not significantly alter the T_g value as long as the sugar type is the same: The reported T_g values for a given type of sugar usually coincide with each other when the matrices are sufficiently dehydrated (Imamura et al., 2006). Surynaranran et al. (Surana et al., 2004) compared three amorphous sugar (trehalose) samples that were prepared by spray-drying, freeze-drying, and melt-and-quench and conclusively confirmed that the method used had no significant impact on the T_g value of an amorphous sugar.

Amorphous sugar matrices are frequently prepared by the melting/quenching of sugar crystals or drying an aqueous solution containing a sugar (Hancock & Zografi, 1997; Hilden & Morris, 2003). On the other hand, we recently reported on a method for preparing an amorphous sugar by the evaporation of a solution of the sugar in an organic solvent (Satoh et al., 2016). A sugar in the amorphous state can be homogeneously dissolved in an organic solvent such as methanol, without the need for a surface active agent, although it is usually temporal (e.g. 2 min for sucrose; >10 days for α-maltose). The organic solution of a sugar can be taken to dryness before the sugar is segregated, resulting in the formation of an amorphous sugar matrix that originated from an organic solvent (Satoh et al., 2016). When hydrophobic substances such as fat-soluble flavors and water-insoluble drugs are preliminarily dissolved in an organic solvent, an amorphous sugar matrix that can disperse hydrophobic substances at the molecular level is produced by drying the mixed solution of the sugar and hydrophobic substance (Satoh et al., 2016, Takeda et al., 2017). These series of procedures may provide an alternative technique for preparing an amorphous solid dispersion (Leuner & Dressman, 2000; Ilevbare et al., 2013; Li et al., 2013; Huang & Dai, 2014) resulting in an improved aqueous dissolution and thus the bioavailability of the hydrophobic drugs. This Sole-Amorphous-Sugar-based Solid Dispersion (SAS-SD) does not require the use of any surface active agent and was demonstrated to significantly improve the aqueous dissolution behavior of BCS class II drugs (Indomethacin, ibuprofen, gliclazide, nifedipine) (Takeda et al., 2017). However, surprisingly, the matrix obtained from an organic solvent (methanol), showed a markedly (~50˚C) lower T_g than that from an aqueous solution, which is a serious drawback to its use as pharmaceutical formulations.

In this study, we investigated the mechanism, by which an organic solvent lowers the T_g of an amorphous sugar. The amorphous sugar matrix was prepared by drying a

solution of the sugar dissolved in an organic solvent. The properties of the product compared with a sample prepared by freeze-drying from water, with respect to the hydrogen bonding state of sugar molecules as well as the T_g value. α-Maltose and methanol were used as a representative sugar and an organic solvent, respectively. The molecular conformation of α-maltose in methanol was semi-quantitatively estimated and compared with that in water. In the process of these investigations, it was found that the T_g value of the amorphous sugar matrix obtained from methanol could be significantly increased as the result of heating. Hence, the methanol-originated amorphous sugar samples were heated under different conditions including temperature and heating period and infrared spectra were obtained as well as T_g values. Finally, the influence of the heat-treatment on the aqueous dissolution behavior of hydrophobic drugs from the SAS-SD was investigated.

3.2. Materials and Methods

3.2.1. Materials

α-Maltose and methanol were purchased from Wako Pure Chemical Industries, Ltd., (Osaka, Japan). Curcumin (Sigma), indomethacin (γ-form of the crystal, Wako Pure Chemicals), and ibuprofen (Wako Pure Chemical Industries) were employed as hydrophobic drugs. All of these chemicals were of reagent grade and were used without any purification.

3.2.2. Preparation of Amorphous Sugar Matrix from Methanol and Heat Treatment

An amorphous sugar cake, which had been freeze-dried from an aqueous solution and then thoroughly dehydrated (Imamura et al., 2008) to below 0.002 g/g-dry matter (Takeda et al., 2017), was dissolved in methanol to give a final concentration of 100 mg/mL. In some cases, a hydrophobic model drug (curcumin, ibuprofen, or indomethacin) was dissolved in the methanol solvent at a concentration of 1 mg/mL. Immediately thereafter, a 100 μL aliquot of the sample was transferred to a 1.5 mL-polypropylene tube and dried at 30±1˚C for 60 min under a pressure of ca. 1 Torr in the presence of an applied centrifugal force (initial drying). After a 60 min period of initial drying, the residue was punctured with a steel needle (Hidaka et al., 2018), followed by the secondary vacuum

drying for an additional 30 min (Takeda et al., 2017). The subsequent vacuum drying reliably induced foaming and enabled complete desolvation (<0.001 g-methanol/g-dry matter) (Takeda et al., 2017).

The obtained dried sample was alternatively transferred in a glass vial and then heated in a drying oven. The heating temperature and period were varied from 30 to 120˚C and from 0 to 120 min, respectively. Immediately after the heat treatment, the heated SAS-SD samples were withdrawn from the glass vial and then analyzed for their physicochemical characteristics as described below.

3.2.3. Differential Scanning Calorimetry

Differential scanning calorimetry (DSC) analyses of amorphous sugar matrices, obtained from methanol as well as water, were carried out, using a TA Q2000 calorimeter (TA instruments Co., New Castle, DE) equipped with RCS90 cooling system (TA instruments Co.) in the same procedures as was used in our previous study (Kinugawa et al., 2015). In brief, a few mg amorphous sugar sample was hermetically sealed in an aluminum pan and then scanned at a rate of 10˚C/min between -40 and 190˚C, using an empty aluminum pan as a reference. From the obtained DSC curves, the T_g of the sample was determined as the onset of the corresponding thermal event.

3.2.4. Fourier Transform Infrared Ray Spectroscopy

IR spectra for amorphous sugar samples were measured by means of a diffuse diffraction method using a Fourier transform IR spectrometer (FTIR, Magna 560, Nicolet Co., Madison, WI) in the same manner as was used in our previous study (Imamura et al., 2008). Namely, a 1~2 mg sample of amorphous sugar was mixed with more than a 50-fold amount of powdered KBr using an agate mortar and pestle in a globe bag filled with nitrogen gas and then packed in a stainless steel cup, which was then set in the diffuse reflection attachment (Gemini, Spectra Tech., Co., Shelton, CT) equipped with the FTIR. The IR spectra were scanned 64 times from 600 cm^{-1} to 4000 cm^{-1} at a resolution of 2 cm^{-1}.

In order to semi-quantitatively estimate the extent of formation of hydrogen bonding of sugar molecules in the amorphous matrices, the sugar O-H stretching vibration bands of amorphous sugar samples were analyzed for the peak wavenumbers. The IR band

due to sugar O-H stretching vibration at around 3300 cm^{-1} was smoothed at 80 points to determine the peak wavenumber.

The FTIR analyses were carried out at least in triplicate for each sample, and the deviations in wavenumber was within 5 cm^{-1} of the average values.

3.2.5. Specific Molar Volume Analysis

Precisely 10 mL of methanol or water was placed in a 20 mL graduated cylinder, and 0.1~2 g (0.3~6 mmol) of the freeze-dried amorphous α-maltose cake was then added to the measured solution (methanol or water) in the graduated cylinder. The amorphous α-maltose cake was completely dissolved by gently inverting the graduated cylinder several times. After removing the bubbles on the cylinder wall, the change of the volume (dV) was determined and converted to the apparent partial mole volume of sugar (v_{sugar}) by being divided by the amount of the added sugar (n mol) (Eq. (1)).

$$v_{sugar} = dV/n \qquad (1)$$

3.2.6. Dissolution Behavior of Hydrophobic Drugs from SAS-SDs

The drug release behavior of amorphous sugar matrix is essential as a drug carrier of solid dispersion and may possibly change as the result of above-mentioned heat treatment of the SAS-SD. Hence, the drug dissolution behavior from the SAS-SDs with and without the heat treatment was analyzed. Namely, the SAS-SDs (model drug content: 1wt%), heated at 120˚C, as well as without being heated were suspended (dissolved) in a known amount of water at 37±1˚C and then stirred at 200 rpm with a 1.5-cm magnetic stirring bar. The amounts of hydrophobic drugs added to the water were 10 μg/mL for curcumin, 100 μg/mL for ibuprofen, and 500 μg/mL for indomethacin. In the cases of ibuprofen and indomethacin, a 200~1,000 μL aliquot of the suspension was withdrawn and then filtered with 0.2 μm pore size filter (Nihon Millipore K.K., Tokyo, Japan) to remove insoluble aggregates. The concentration of the dissolved ibuprofen and indomethacin was determined by measuring the UV-vis absorption intensity at specific wavelengths (ibuprofen: 233 nm; indomethacin: 318 nm). When curcumin was used as a model hydrophobic drug, the area of UV-vis absorption of 300-400 nm of the water-suspended sample ($A_{300\text{-}400}$) was measured, in which the filtration of the withdrawn

aliquot was omitted because it induced a significant degree of aggregation of curcumin. The dissolved curcumin concentration in water was calculated using the conversion factor (7.75 Abs•nm/(μg/mL)) that had been preliminarily determined from the relationship between the $A_{300\text{-}400}$ (at 10 μg/mL curcumin) and the water/ethanol solvent composition.

3.3. Results and Discussion

3.3.1. Why does an Organic Solvent Lower the T_g of an Amorphous Sugar Matrix?

Fig. 3.3.1 shows DSC thermograms of sugar matrices obtained by vacuum foam drying from a methanol solution as well as drying from an aqueous solution (by freeze-drying). No endothermic peak was detected for the methanol-originated sample due to the evaporation of the remaining methanol, indicating that a nearly complete desolvation occurred during the vacuum foam drying. A single heat capacity shift due to a glass-to-rubber transition and no endothermic peak corresponding to the melting of sugar crystals were detected for the amorphous α-maltose that was dried from methanol, as well as the water-originated sample (Fig. 3.3.1). The magnitude of the heat capacity shift due to the glass-to-rubber transition (ΔC_p) for the amorphous sugar samples was estimated from the DSC curves and are shown along with the corresponding T_g values in Table 3.3.1. The ΔC_p value for the amorphous sugar dried from an aqueous solution is consistent with reported values for the samples prepared by melting/quenching (Orford et al., 1990; Roos, 1993). It should be noted that the ΔC_p for the methanol-originated sample is markedly smaller than that for the water-originated sample. This suggests that the enthalpy level of the methanol-originated sugar matrix is lower than that of the water-originated sample.

IR spectra for the amorphous sugar matrices dried from methanol and water were measured (Fig. 3.3.2), indicating that the peak position of the absorption due to O-H stretching vibration for the methanol-originated sample (3307±3 cm^{-1}) is much lower than that for the water-originated sample (ca. 3328±3 cm^{-1}), as listed in Table 3.3.2. Considering that hydrogen bond formation lowers the O-H stretching vibration frequency of sugar molecules, it can be deduced that more sugar-sugar hydrogen bonding had formed in the amorphous sugar matrix dried from methanol than in that from water. The high degree of hydrogen bonding may lower the enthalpy of the amorphous sugar matrix, which coincides with the markedly small ΔC_p for the methanol-originated sample (Table

3.3.1).

The volume of the methanol solutions containing different amounts of amorphous sugar (α-maltose) as well as those for the aqueous solution were measured and the values are shown in Fig. 3.3.3 as a function of the amount of added sugar. As shown in Fig. 3.3.3, the slope for the increase in the methanol solution volume with the amount of sugar is markedly smaller than that for the aqueous solution volume. From Fig. 3.3.3, the apparent molar volumes of α-maltose in methanol and water were calculated to be 158 and 220 mL/mol, respectively. The value for water is consistent with previously reported values (Banipal et al., 1997; Zhuo et al., 2005). It should be emphasized that the volume occupied by each sugar molecule in methanol is estimated to be approximately 30% smaller than that in water.

A sugar molecule in a poor solvent may change its conformation so as to decrease the surface area that is in contact with the solvent. The lower permittivity of methanol than that of water would be expected to allow intramolecular hydrogen bonding in disaccharide molecules, which would also reduce the occupied volume of a sugar molecule. Consequently, the partial molar volume of α-maltose in methanol appears to be substantially smaller than in water, as shown in Fig. 3.3.3.

Considering these findings, the following mechanism is proposed for markedly lower T_g of the amorphous sugar matrix, dried from methanol. First, the sugar molecules in the methanol-originated matrix may, more or less, maintain their compact conformation in methanol. Therefore, the molecules in the methanol-originated matrix would have a smaller mean intermolecular distance and thus a greater degree of hydrogen bonding, as indicated by the lower frequency of sugar O-H stretching vibration (Table 3.3.2). It would consequently follow that the smaller volume assigned to each sugar molecule would lowers the T_g where the free volume of sugar molecule reaches a critical value (Fig. 3.3.1).

The findings of this study demonstrate that the type of solvent used can significantly alter the T_g value for a dried amorphous sugar matrix, which is noteworthy because, in the past, the T_g of amorphous sugar matrix has been assumed to be unchanged, irrespective of the preparation method and conditions (Imamura et al., 2006; Surana et al., 2004). The influence of the solvent type appears to be closely related to the conformation of sugar molecules in the dried matrix, as described above. These findings

point to the possibility of an alternative methodology for use in controlling the physicochemical characteristics of an amorphous sugar solid.

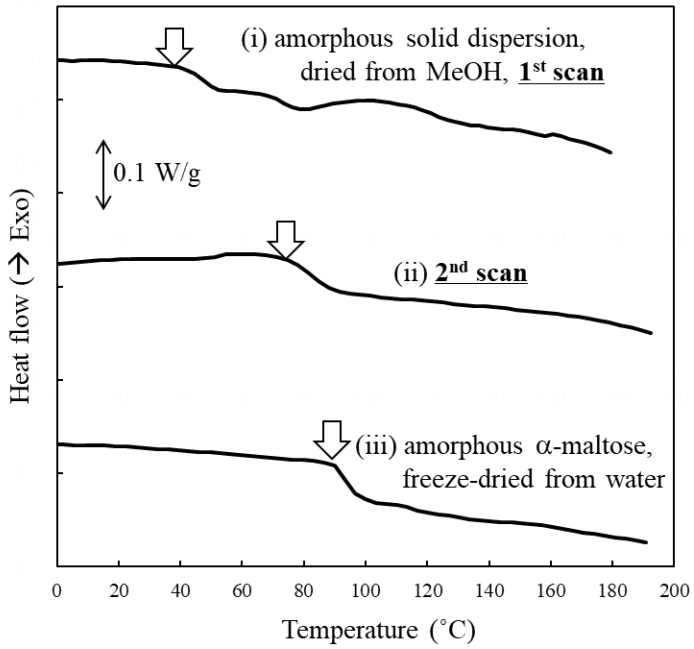

Fig. 3.3.1. DSC thermograms for (i) amorphous α-maltose, vacuum-dried from methanol, and (ii) the second heating as well as (iii) amorphous α-maltose, freeze-dried from water. Arrows in the graph denote T_g values. The amounts of solvent remaining in samples dried from methanol and water were both at negligible levels (below 0.001 and 0.002 g/g-dry matter, respectively[35]) .

Table 3.3.1. Apparent heat capacity change (ΔC_p) upon glass-to-rubber transition of amorphous sugar (α-maltose), prepared by different methods. T_g values are also shown.

Preparation method	ΔC_p ($Jg^{-1}K^{-1}$)	T_g (˚C)
Dried from methanol	0.274±0.102[a]	36±1[35]
Freeze-dried from water	0.691±0.069[a]	90±1,[35] 87[44]
Melting/quenching	0.79,[20] 0.61[45]	96,[20] 86[45]

[a]This study

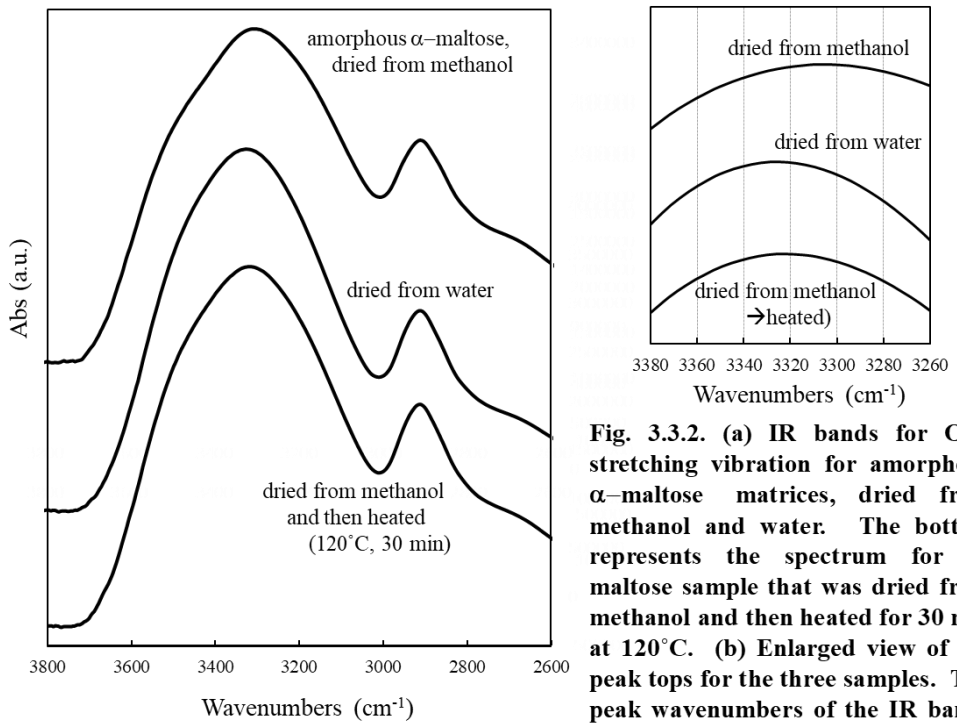

Fig. 3.3.2. (a) IR bands for O-H stretching vibration for amorphous α–maltose matrices, dried from methanol and water. The bottom represents the spectrum for α-maltose sample that was dried from methanol and then heated for 30 min at 120˚C. (b) Enlarged view of the peak tops for the three samples. The peak wavenumbers of the IR bands are shown in Table 1.

Table 3.3.2. Peak wavenumbers of O-H stretching vibration band for amorphous α-maltose samples, dried from methanol, freeze-dried from water, and dried from methanol → heated for 30 min at 120˚C.

Dried from	Wavenumber (cm^{-1})
methanol	3307±3
water	3328±3
methanol→ heat treatment	3323±2

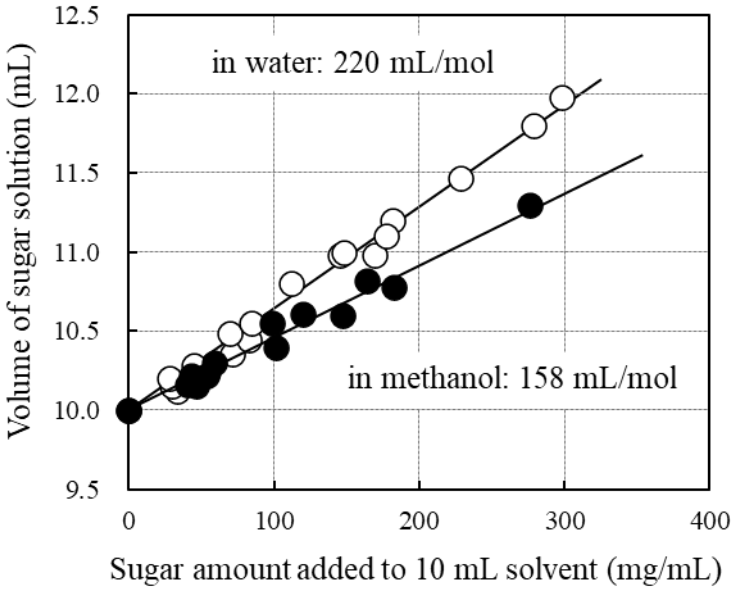

Fig. 3.3.3. Increases in the volume of aqueous (open circles) and methanol solutions (closed circles) as a function of sugar amount added to the solution at 20˚C. Freeze-dried amorphous α-maltose was added to 10 mL water or methanol. The apparent partial molar volumes of α-maltose in water and methanol were calculated and are indicated in the graph.

3.3.2. Influences of Heat Treatment on SAS-SD

As shown in Fig. 3.3.1, when the methanol-originated sugar matrix was scanned twice, the T_g value was markedly increased, suggesting that the thermal treatment improved the physical stability of the sugar matrix dried from methanol. Hence, the influence of temperature and the duration of heating on the methanol-originated sample were investigated.

The T_g values for amorphous α-maltose, dried from methanol and then heated under different conditions, were measured and the results are shown against heating period (at 120˚C) and temperature (for 60 min) in Figs. 3.3.4 (a) and (b), respectively. As shown in Fig. 3.3.4 (a), T_g increases with time and then reaches a maximum value that is slightly (ca. 10˚C) lower than the value for the water-originated sample (ca. 90˚C). The shape of the time dependence curve for T_g (Fig. 3.3.4 (a)) is indicative of a typical relaxation process from the unstable state to the stable one, stimulated by heating. Figure 3.3.4 (b)

shows that the T_g increases with increasing temperature, which becomes especially significant at a temperature of around 50˚C. This may be related to the fact that this temperature range (~50˚C) is positioned between the two T_g values for the methanol- and water-originated amorphous α-maltose matrices (ca. 36˚C and 90˚C, respectively).

The IR peak frequencies of sugar O-H stretching vibration for amorphous α-maltose dried from methanol was measured also after heating at 120˚C for 60 min, indicating the wavenumber close to that for the sample freeze-dried from water (Table 3.3.2). This coincides with the fact that the T_g value reached that for the water-originated sample as the result of 60-min heating at 120˚C (Figs. 3.3.4) and suggests that the heat treatment results in a loss of hydrogen bonding.

As indicated by Table 3.3.2 and Fig. 3.3.3, the sugar molecules in the amorphous sugar matrix, originated from methanol, may have a considerably small occupied volume and have a markedly high degree of hydrogen bonding. Such a conformational state of a sugar molecule may distort its molecular structure. The mitigation process of the molecular distortion would be, as indicated by Fig. 3.3.4 (a), a type of relaxation that would require cooperative movements of the surrounding sugar molecules. The conformational relaxation of sugar molecules in the methanol-originated amorphous matrix is therefore considered to become significant at temperatures above the T_g value (ca. 36˚C), resulting in marked increases in the T_g (Fig. 3.3.4 (b)).

The SAS-SD samples, containing model hydrophobic drugs (ibuprofen, indomethacin, and curcumin), were prepared from methanol solutions and then heated at 120˚C for 60 min. The dissolution profiles of hydrophobic drugs in water from the heat-treated SAS-SD sample as well as from the unheated samples were then measured (Figs. 3.3.5 (a-c)). Both the heated and unheated SAS-SD samples exhibited typical “spring and parachute” dissolution curves (Brouwers et al., 2009). Namely, the concentration of the dissolved drug increases up to much above the equilibrium solubility at the early stage (“spring”) and then decreases to reach an equilibrium value (“parachute”), whereas the crystalline drug shows a gradual increase toward saturation. As shown in Figs. 3.3.5, the heat treatment affects the aqueous dissolution behavior differently and is dependent on the drug type. As shown in Figure 3.3.5 (a), when ibuprofen was used as a model hydrophobic drug, the heat treatment increased the attained maximum dissolved concentration by 20~30% relative to the maximum for the unheated sample. In the case

of indomethacin, the decrease in the dissolved indomethacin concentration after the "spring" is markedly decreased as the result of the heat-treatment although the attained maximum dissolved concentration is slightly lower. However, the maximum dissolved concentration for curcumin was decreased by the heat treatment. The "parachute" of the dissolved curcumin concentration also is enhanced due to the heat treatment. These findings demonstrate that the heat-treatment of the SAS-SD, originating from a methanol solution, can improve the extent of aqueous dissolution of hydrophobic drugs, although not in all cases.

It has been reported that, in the aqueous dissolution of hydrophobic drugs from polymer-based amorphous solid dispersion, the dissolved polymer often inhibits crystallization of supersaturated drug molecules and extend the supersaturation state of the drug (Huang & Dai, 2014; Sun & Lee, 2010; Liu et al., 2016; Taylor & Zhang, 2016). Considering this, the following explanation may be possible for the marked extension of the attained dissolved state of ibuprofen and indomethacin as the result of heat treatment (Fig. 3.3.5 (a) and (b)). Namely, the cooperative relaxation of the sugar conformation due to heating may lead to the exclusion of the embedded drug molecules into the spaces among the sugar matrix domains consequently resulting in the formation of drug aggregates, possibly so small as to be accounted for as dissolved drugs in the dissolution profile measurements. Another effect of the heat treatment at 120˚C may be to prevent the structural ordering (crystallization) of the aggregated drug molecules (the melting points are ca 76˚C for ibuprofen and 153-160˚C for indomethacin). Consequently, the microscopic and amorphous drug aggregates could be stably dispersed in the aqueous solution without inducing the crystallization of the drug, as shown in Fig. 3.3.5 (a) and (b). On the other hand, judging from the markedly high melting point of curcumin (180˚C), the heat treatment may possibly allow the curcumin aggregates formed by the heat-induced cooperative relaxation of sugar to undergo crystallization. The crystalline curcumin aggregates would be expected to facilitate the crystal growth in the dissolution test and as a result, the aqueous dissolution of curcumin from the SAS-SD may be lowered as the result of the heat treatment, as shown in Fig. 3.3.5 (c).

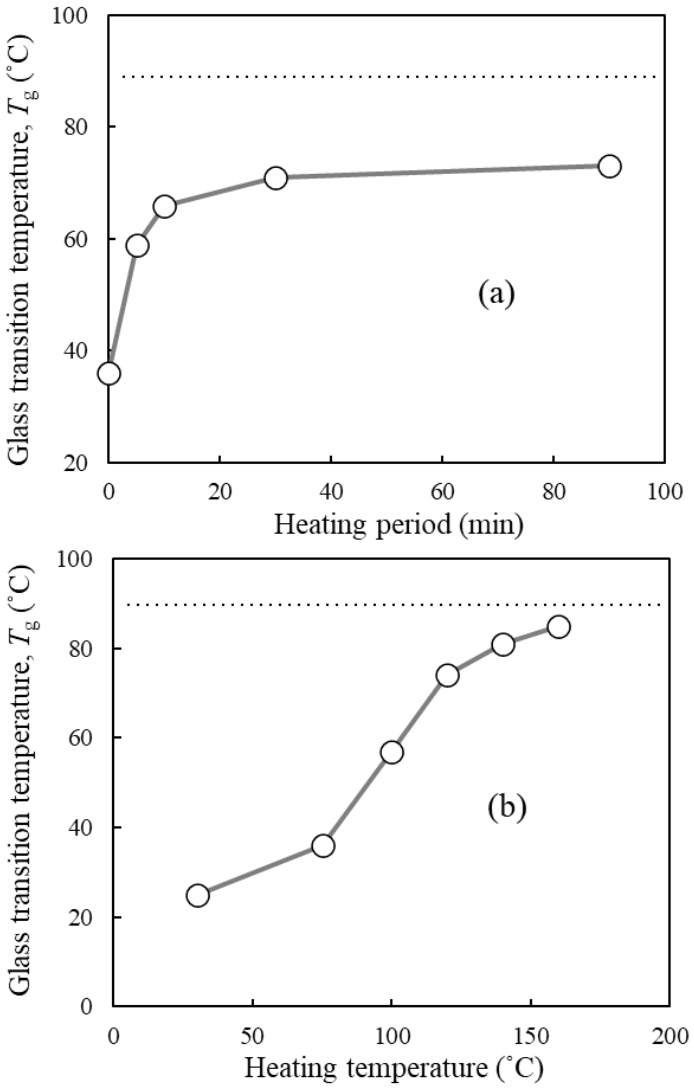

Fig. 3.3.4. Influence of (a) heating period and (b) temperature on T_g values for amorphous α-maltose, obtained from methanol. The T_g value for amorphous α-maltose, obtained by freeze-drying an aqueous solution, is also shown as dotted line. The amounts of solvent remaining for the methanol- and water-originated samples were both at negligible levels (below 0.001 and 0.002 g/g-dry matter, respectively).[35]

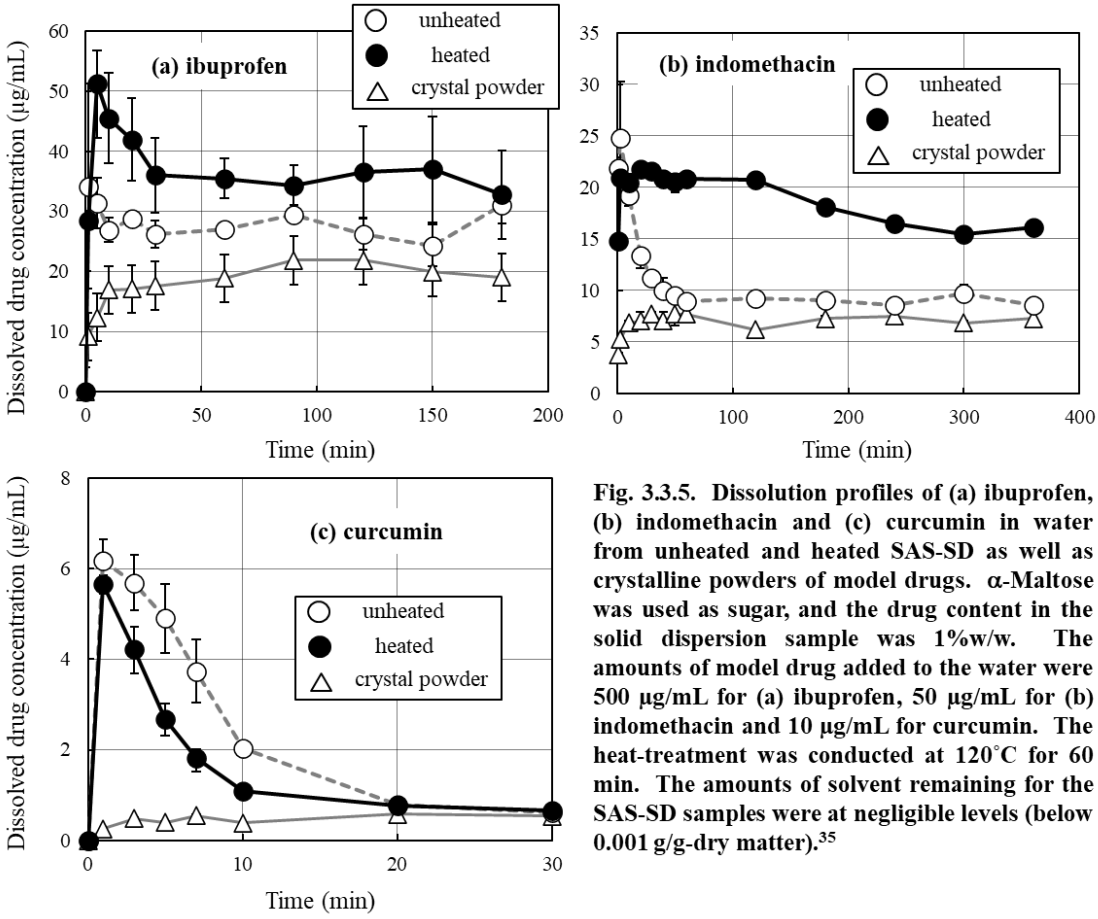

Fig. 3.3.5. Dissolution profiles of (a) ibuprofen, (b) indomethacin and (c) curcumin in water from unheated and heated SAS-SD as well as crystalline powders of model drugs. α-Maltose was used as sugar, and the drug content in the solid dispersion sample was 1%w/w. The amounts of model drug added to the water were 500 μg/mL for (a) ibuprofen, 50 μg/mL for (b) indomethacin and 10 μg/mL for curcumin. The heat-treatment was conducted at 120˚C for 60 min. The amounts of solvent remaining for the SAS-SD samples were at negligible levels (below 0.001 g/g-dry matter).[35]

3.4. Conclusions

An amorphous sugar matrix can be produced by drying an organic (methanol) solution of a sugar as well as by the dehydration of an aqueous sugar solution. However, the glass transition temperature (T_g) of the amorphous sugar dried from methanol was found to be much lower than that from water irrespective of the fact that desolvation from the amorphous sugar matrix was nearly complete. In this study, the markedly low T_g of the methanol-originated amorphous sugar suggests that the conformation of the sugar molecule had become more compact in the dried amorphous matrix. The specific characteristics of the methanol-originated amorphous sugar were reduced due to heating: The T_g and degree of hydrogen bonding for amorphous α-maltose, dried from methanol, were respectively increased and reduced close to those for the water-originated one as the result of heating under appropriate conditions. A heat treatment was found to improve the aqueous dissolution of ibuprofen and indomethacin from the SAS-SD that had been obtained by drying from methanol. However, in the case of curcumin, the aqueous dissolution behavior from the SAS-SD due to the heat treatment was the opposite. Considering these findings, the heat treatment of the SAS-SD is assumed to bring further improvements to the SAS-SD, dried from an organic solvent, although the improvement of the aqueous dissolution behavior of hydrophobic drug may be limited, depending on the drug type under consideration.

Chapter 4 Water Sorption and Glass-to-Rubber Transition Characteristics of Amorphous Sugar Matrices, Dried from Alcohols under Different Conditions

4.1. Introduction

An amorphous phase comprised of sugar is often found in food and pharmaceutical products and plays an important role in the functionality and quality of the final products (Cassanelli et al., 2018**;** Chen, 2007;Yu, 2001.). Another important aspect of amorphous sugar is the fact that it can be used to stabilize unstable ingredients (Crowe et al., 1984; Desai & Park, 2005; Manning et al., 1989; Pikal, 1994; Shimada et al., 1991). Amorphous sugar matrices can be used to encapsulate other molecules and protect them against chemical degradation (Kuang et al., 2015; Zhou & Roos, 2012.) physicochemical change (van Drooge et al., 2004; Palomaki et al., 2020) and aggregation (Alkilany et al., 2014; Liu et al., 1991). However, an amorphous sugar is not in a stable equilibrium and has a tendency to turn into a rubbery paste-like substance, which can then subsequently form a crystalline solid, as the result of water sorption, increasing temperature, or a combination thereof (Buera et al., 2005; Harnkarnsujarit & Charoenrein, 2011; Kedward et al., 2000b). It naturally follows that an amorphous sugar phase can lose its functionalities in food and pharmaceutical products.

Due to the usability and instability of amorphous sugars, there have been numerous reports on the water sorption behavior (Hancock & Dalton, 1999; Imamura et al., 2010a; Liu et al., 2006), glass transition temperature (T_g) (Liu et al., 2006; Schebor et al., 2010; Slade & Levine, 1988), and the relationship between them (Li, 2022; Roos & Karel, 1991b, 1991c; Roos, 1993) as well as crystallization behavior (Heljo et al., 2012; Kedward et al., 2000b; Schebor et al., 2010). In particular, data sets of T_g and the amount of sorbed water at given RHs have been reported for most of the commercially available sugars (Heljo et al., 2012; Imamura et al., 2010a; Jouppila & Roos, 1994; Orford et al., 1990; Roos, 1993; Roos & Karel, 1991b). As a result, it is generally accepted that increasing the RH which is accompanied by the amount of sorbed water lowers the T_g value of an amorphous sugar matrix by exerting a plasticizing effect on the sorbed water (Roos & Karel, 1991b). The dependence of the T_g value of an amorphous sugar on the amount of sorbed water generally tends to shift toward higher temperature with increasing molecular size of the sugar of interest (Imamura et al., 2010; Orford et al., 1990; Roos,

1993). In addition, even with the same molecular weight, the monomer structure (e.g., glucopyranose, fructofuranose, etc.) and the linkage position matters and these factors can result in markedly different glass(-to-rubber) transitions (Imamura et al., 2006) and water sorption behavior (Bogdanova et al., 2021; Imamura et al., 2010a).

In contrast to the above findings, the reported T_g values and water sorption isotherms of an amorphous sugar matrix are usually quite consistent with each other, even when they were determined by different research groups and even under different conditions. This indicates that the physicochemical properties of an amorphous sugar matrix would be independent of the conditions used in its preparation. Actually, matrices of amorphous trehalose were prepared by different methods, namely, freeze-drying, spray-drying, and melt/quench, and found to have the almost the same T_g values in the thoroughly dehydrated state (Surana et al., 2004).

On the other hand, we recently developed a new technique for preparing amorphous sugar matrices (Satoh et al., 2016). While an amorphous sugar matrix is usually obtained by drying an aqueous solution of a sugar or by quenching the melted sugar; when certain types of disaccharides are amorphized, it becomes possible to dissolve them in methanol and ethanol for a short time (before segregation occurs) and further drying them into an amorphous dry powder (Satoh et al., 2016). This technique which is based on dissolving the sugar alcohols, can then be used for preparing a Sole-Amorphous-Sugar-base Solid Dispersion (SAS-SD) of hydrophobic substances in an amorphous sugar matrix (Okamoto et al., 2022; Satoh et al., 2016; Sekitoh et al., 2021a; Takeda et al., 2017; Takeda et al., 2019).

Using the above technique, we actually prepared amorphous matrices of sugars from methanol or ethanol, in which vacuum foam drying (Arevalo-Pinedo & Murr, 2006; Hidaka et al., 2018; Wu et al., 2007) was employed as a drying method. The prepared amorphous sugar matrices were analyzed for their glass(-to-rubber) transition and crystallization behavior (Sekitoh et al., 2021b; Takeda et al., 2019). The results indicated that the T_g value was markedly lowered (Takeda et al., 2019) and that crystallization propensity was clearly enhanced, relative to those of the amorphous sugar that were dried from an aqueous solution (Sekitoh et al., 2021b). The extent of hydrogen bonding between sugar molecules in the alcohol-originated amorphous matrix was also evaluated from the O-H stretching vibration frequencies (Sekitoh et al., 2021b; Takeda et

al., 2019). The results indicated that more sugar-sugar hydrogen bonds were formed in the alcohol-originated amorphous sugar matrix than in that obtained from an aqueous system (Takeda et al., 2019). These collective results demonstrate that the physicochemical characteristics of an amorphous sugar matrix strongly appears to depend on the type of solvent being used.

This study focuses on the impact of solvent type and drying method on the glass(-to-rubber) transition and water sorption behavior of an amorphous sugar matrix as well as the relationship between them. α-Maltose, palatinose, trehalose and maltitol were used as model sugars, and methanol and ethanol were used as solvents. Two drying methods, vacuum foam drying (Arevalo-Pinedo & Murr, 2006; Hidaka et al., 2018; Wu et al., 2007) and spray drying, were employed to dry the alcohol solutions. The alcohol-originated amorphous sugar samples, prepared under different conditions, were thoroughly dried or/and moistened at specified RHs, and the T_g value and amount of water sorbed in the samples were measured. The obtained relationship between T_g and the amount of sorbed water for the alcohol-originated samples were compared with those for aqueous freeze-dried (amorphous) sugars as well as between the two drying methods. IR absorption spectra of the samples were also collected and used to evaluate the degree of hydrogen bond formation in the amorphous sugar samples. Based on the obtained results, we discuss how the solvent type as well as drying method affects the physicochemical characteristics of an amorphous sugar matrix.

4.2. Materials and Methods

4.2.1. Materials

Methanol and ethanol, used as solvents, were obtained from Nacalai Tesque Inc. (Kyoto, Japan). α-Maltose, palatinose, and trehalose were products of Fujifilm Wako Pure Chemical Co. (Osaka, Japan). P_2O_5, LiCl, CH_3COOK, and $MgCl_2$ were obtained from Wako Pure Chemical Industries. All of these chemicals were of reagent grade and were used without further purification.

4.2.2. Preparation of Amorphous Sugar Samples

4.2.2.1. Freeze-Drying of Aqueous Sugar Solution

Powdered crystalline sugar was dissolved in distilled water to a final concentration of 100 mg/mL. In the cases of α-maltose and palatinose, a 10 mL aliquot of the prepared aqueous solution was instantaneously frozen with liquid nitrogen. The aqueous solution of trehalose was frozen in 10 mL aliquots by placing the samples in a freezer (-20˚C) for 60 min and further in liquid nitrogen for ~5 min, according to previously reported findings (Sekitoh et al., 2021b). The frozen solutions were subjected to freeze-drying, yielding fully amorphous sugar cakes (Imamura et al., 2010a). The freeze-dried amorphous sugar cakes were stored in a vacuum desiccator over P_2O_5 at 30˚C for more than three days to ensure that they were thoroughly dehydrated to the detection limit (>0.002 g/g-dry matter) (Imamura et al., 2010a). The resulting thoroughly dehydrated amorphous sugars were analyzed as they were (aqueous freeze-dried amorphous sugar) or were used for the preparation of vacuum-foam- and spray-dried amorphous sugar samples, as described below.

4.2.2.2. Vacuum Foam Drying of Alcohol Solution

One gram of a thoroughly dehydrated amorphous sugar sample was vigorously stirred with 10 mL of methanol or ethanol, using a vortex mixer (for ~10 seconds), to be fully dissolved. Immediately thereafter, 100 μL aliquots the alcohol solution of the dissolved sugar, was dispended in polypropylene 1.5 mL tubes and then vacuum-foam-dried, following the procedure that had been established previously (Fujioka et al., 2022; Hidaka et al., 2018). Namely, the dispensed aliquots of the sample solution first were subjected to reduced pressure (~2,000 Pa) with a centrifuge (3250 rpm, 473g) for 60 min (initial drying), using a EYELA CVE-1010 centrifugal concentrator (TOKYO RIKAKIKAI Co., Tokyo, Japan) connected to an ULVAC FDU-1200 diaphragm type vacuum pump (ULVAC Japan, Ltd., Tokyo, Japan). The initial drying did not induce the foaming of the sample solution. After the initial drying, the partly dried sample solutions were punctured with a stainless steel needle (Hidaka et al., 2018), followed by further drying under reduced pressure (~2,000 Pa) (Secondary drying). The (start of the) secondary drying reliably induced foaming of the remaining sample solutions, which became the

vacuum-foam-dried samples (Fujioka et al., 2022; Tramis et al., 2022).

In this study, water as a solvent and a combination of trehalose and ethanol were not employed for the vacuum-foam-drying because of difficulties associated with identifying the effective needle stimulation conditions (initial drying period) and the shortness of the duration where the full dissolution of trehalose in ethanol was maintained, respectively.

4.2.2.3. Spray Drying of Alcohol Solution

Methanol solutions, containing 100 mg/mL sugar (α-maltose and palatinose), were prepared in the same manner as that for the vacuum foam drying (2.2.2.) and immediately then introduced into a Yamato ADL-311S spray-dryer (Yamato Scientific Co., Ltd., Tokyo, Japan). The introduced sample solution was sprayed from a two-fluid nozzle atomizer, in which the feed rate and atomization gas pressure were 3.5 mL/min and 0.1 MPa, respectively, and dried by 0.68 m^3/min downstream hot air. The inlet temperature of the hot air (T_{inlet}) was set to 60˚C or 180˚C, for which the outlet temperatures was 41±1˚C or 105±3˚C, respectively. The spray dried particles were separated in a glass cyclone and collected. In the preliminary step of this study, the remaining amount of solvent of the spray-dried sugar sample had been gravimetrically determined to be around 0.05 g/g-dry matter and found not to give a further decrease even by a vacuum drying using the above-mentioned freeze-dryer (section 2.2.1.). This was deduced to result from the formation of a dense “skin” layer of concentrated solute (sugar) on the spray dried particle/droplet and the subsequent barrier against further evaporation of the remaining solvent (Paramita et al., 2010). Hence, we decided that, prior to the characterization and humidification of the spray-dried samples (sections 2.3., 2.4), the spray-dried sugar particles were ground with an agate mortar and pestle adequately (3 min) in a glove bag filled with N_2 gas and then stored in a vacuum desiccator over silica gel (25˚C) for more than 3 days. According to the gravimetric analyses, the additional treatments (grinding and drying over silica gel) was confirmed to successfully remove the remaining solvent from the spray-dried samples to less than 0.01 g/g-dry matter.

In this spray-drying process, water and ethanol could not be used as a solvent due to the difficulties in finding the process conditions needed to maintain the dissolved state of sugars throughout the process (~30 min), respectively. Furthermore, the subsequently-described thermal analysis (section 2.3.) indicated that trehalose dissolved in methanol

occasionally resulted in partial crystallization during the spray-drying. Consequently, the spray-drying was limited in this study to the two combinations of α-maltose/methanol and palatinose/methanol.

4.2.3. Water Sorption by Amorphous Sugar Sample

The amorphous sugar samples, prepared (and further dried) as described above, were stored in a vacuum desiccator over saturated solutions of LiCl, CH_3COOK, and $MgCl_2$ for more than three days. The equilibrium relative humidities (%) over saturated LiCl, CH_3COOK, and $MgCl_2$ solutions were 11%, 23%, and 33%, respectively (Greenspan, 1977). The sorption of water by the amorphous sugar samples had been preliminarily confirmed to reach the maximum within 3 days.

Some part of the humidified amorphous sugar sample was quantified for the extent of water sorption by the Karl-Fischer titrimetric method, in the same manner as in our previous study (Imamura et al., 2001) (The other was analyzed for the T_g value as described below). The measurement of the sorbed water amount was at least done in triplicate for each sample.

4.2.4. Differential Scanning Calorimetry

Differential scanning calorimetry (DSC) analyses of the amorphous sugar samples, prepared by different drying methods and conditions (section 2.2.1~2.2.3) and then humidified at different RHs (section 2.3), were conducted following the same procedures as that in our previous study (Kinugawa et al., 2015). Namely, a few mg of the prepared sugar sample was hermetically packed in an aluminum pan and then scanned at a rate of 10°C/min between -50°C and 190°C with an empty reference pan. From the obtained DSC curves, the onset temperature and the magnitude of the shift in the heat capacity change due to a glass-to-rubber transition were read as the T_g (˚C) and the corresponding heat capacity change, ΔC_p (J/(g•K)), respectively.

In a usual DSC analysis, a preparatory heating (upward scan) of an amorphous material is carried out before each measurement of the thermogram for the purpose of eliminating the influence of enthalpy relaxation of the amorphous material, including the overestimation of T_g (Fox & Flory, 1950; Tant & Wilkes, 1981). However, our previous study revealed that the preparatory heating resulted in a rise in T_g of the alcohol-originated

amorphous sugar (Takeda et al., 2019). Furthermore, the overestimation of the T_g due to enthalpy relaxation generally is not significant below several ˚C. Hence, in this DSC measurement, each prepared sample was scanned only once without and additional preparatory heating.

4.2.5. Fourier Transform Infrared Ray (FTIR) Spectroscopy

IR absorption spectra of amorphous sugar samples that had been dried under different conditions were measured, according to the same procedure as was used in our previous study (Imamura et al., 2008). In brief, a few mg of an amorphous sugar sample was ground into a fine powder with a few hundred mg of powdered KBr and then filled in a stainless steel cup for the diffuse reflection attachment (Gemini, Spectra Tech., Co., Shelton, CT). The 64 FTIR scans were performed for each sample, from 600 cm^{-1} to 4000 cm^{-1} at a resolution of 4 cm^{-1}, using a Nicolet 4700 Fourier transform IR spectrometer (Thermo Scientific Inc., Madison, WI) with a diffuse diffraction technique. The FTIR measurements were performed at least in triplicate for each sample.

In this study, from the obtained IR spectra for each different amorphous sugar sample, the peak position of the sugar O-H stretching vibration band was determined as an index of the sugar-sugar hydrogen bond formation (Imamura et al., 2006; Kagotani et al., 2013). Thereby, the IR absorption bands at around 3300 cm^{-1}, corresponding to sugar O-H stretching vibration, in the measured IR spectra for the amorphous sugar samples were smoothed at 80 points and analyzed for their peak wavenumbers.

4.2.6. Partial Molar Volume of Sugars in Methanol

Partial molar volumes of sugars in methanol as well as water were measured in the same manner as was used in our previous study (Takeda et al., 2019). Namely, prescribed masses of freeze-dried amorphous sugar cake were added and completely dissolved in a fixed volume (10 mL) of methanol or water in a graduated cylinder. The increased volumes (dV mL) of the methanol or water solution were determined for different added masses of the amorphous sugar (n mol). Finally, the slope of the dependence of dV on n were determined as the apparent partial mole volume (mL/mol) of the sugar.

4.3. Results and Discussion

4.3.1. Hydrogen Bonding States of Amorphous Sugar Samples

An amorphous sugar matrix is constructed through intermolecular hydrogen bonds, that are formed randomly between the constituent sugar molecules. The hydrogen bonding states of an amorphous sugar matrix is considered to reflect the molecular packing density (Imamura et al., 2008; Kagotani et al., 2013) and further affect the characteristics of the correponding amorphous matrix, including water sorption and glass-to-rubber transition behavior. Hence, this study first set out to compare the IR peak wavenumbers for sugar O-H stretching vibration bands, $\nu_{O\text{-}H}$, for amorphous sugar samples that were prepared by different routes (Table 4.3.1). As shown in Table 4.3.1, vacuum foam drying from methanol or ethanol leads to the lowest or second lowest $\nu_{O\text{-}H}$ value for each sugar, respectively, whereas the $\nu_{O\text{-}H}$ values of the aqueous freeze-dried sugars are the highest. The $\nu_{O\text{-}H}$ values of the spray dried α-maltose and palatinose are in intermediate ranges between those of the aqueous freeze-dried and of the alcohol vacuum-foam-dried samples. The $\nu_{O\text{-}H}$ value of the spray dried sample appears to be positively shifted when the T_{inlet} is increased from 60˚C to 180˚C.

In a previous study, we compared the partial molar volumes of α-maltose in methanol as well as water and found that α-maltose molecules have more compact conformations in methanol, relative to that in water (Takeda et al., 2019). The methanol-induced compact conformation of the α-maltose molecule was considered to remain significantly even in the dried state, resulting in a higher molecular packing than that for an aqueous freeze-dried sample. A highly packed amorphous sugar matrix may enable greater extent of intermolecular hydrogen bonding, as indicated by the lower $\nu_{O\text{-}H}$ value in Table 4.3.2 (Takeda et al., 2019). Herein, the partial molar volumes of palatinose and trehalose in methanol as well as in water were newly determined and these values were added in Table 4.3.2. The volumes occupied by single palatinose and trehalose molecules in methanol are clearly smaller than those in water, indicating that these molecules have more compact conformations in methanol than in water, which is consistent with the trend with the case of α-maltose. Accordingly, the lower $\nu_{O\text{-}H}$ values and thus higher molecular packing in the amorphous palatinose and trehalose matrices, vacuum foam dried from alcohols, are also considered to be a holdover from the compact molecular

conformation of these sugars in methanol.

In our previous study, we investigated the influence of heating on the physicochemical characteristics of amorphous α-maltose, prepared by vacuum-foam-drying from methanol (Takeda et al., 2019). The results revealed that a 30 min-heating at 120˚C increased the $\nu_{O\text{-}H}$ values of the amorphous samples that had been prepared from methanol, toward the levels of the aqueous freeze-dried sample (Imamura et al., 2012; Kagotani et al., 2013; Takeda et al., 2019). According to this result, it appears that the heating and consequent thermal agitation caused the highly packed amorphous sugar matrix to relax. Here, spray-drying is always associated with the heating of spray dried particles. Therefore, the amorphous α-maltose and palatinose matrices, that had been spray dried from methanol, may be relaxed at the final stage of the spray-drying process, which would naturally be more significant as the T_{inlet} is higher. This may be the reason for the higher $\nu_{O\text{-}H}$ of the spray dried samples compared to those of the vacuum foam dried samples, as shown in Table 4.3.1.

Table 4.3.1. IR peak wavenumbers of sugar hydroxyl stretching vibration bands, $\nu_{O\text{-}H}$ and glass transition temperatures, T_g, of amorphous sugar matrices in the thoroughly dried states. The changes in the heat capacity due to glass-to-rubber transition, ΔC_p, are also listed. The amorphous sugar matrices were prepared under different conditions, including solvent types and drying methods.

sugar	solvent	drying method	$\nu_{O\text{-}H}$ (cm^{-1})	T_g (°C)	ΔC_p ($Jg^{-1}K^{-1}$)
α-maltose	water	FD	3328±3[a]	90±3[a]	0.72±0.05
	methanol	VFD	3307±3[a]	39±1[a]	0.36±0.02
		SD, T_{inlet}: 60°C	3314±4	61±8	0.95±0.03
		SD, T_{inlet}: 180°C	3316±1	74±1	0.83±0.01
	ethanol	VFD	3312±2	39±3	-
palatinose	water	FD	3327±2	65±5	0.61±0.004
	methanol	VFD	3304±3	17±5	0.56±0.03
		SD, T_{inlet}: 60°C	3314±1	39±4	1.06±0.05
		SD, T_{inlet}: 180°C	3322±1	54±1	0.73±0.001
	ethanol	VFD	3309±6	18±2	-
trehalose	water	FD	3328±4[b]	105±5[b]	0.75±0.05
	methanol	VFD	3308±4[b]	44±2[b]	-

[a] Takeda et al., 2019; [b] Sekitoh et al., 2021b

Table 4.3.2. Partial molar volumes, $V_{p.m.}$, of sugars in water and methanol. The known amounts of freeze-dried amorphous sugar (α-maltose, palatinose, or trehalose) were added to 10 mL of water or methanol. The increases in the solution volume were plotted against the added amount of sugar, and the slopes of the plots were determined as the apparent partial molar volumes of sugars.

sugar	in water		in methanol	
	$V_{p.m.}$ (mL/mol)	R^2	$V_{p.m.}$ (mL/mol)	R^2
α-maltose	220[a]	0.997	158[a]	0.993
palatinose	206	0.999	195	0.995
trehalose	226	0.991	182	0.987

[a] Takeda et al., 2019

4.3.2. Water Sorption Behavior of Alcohol-Originated Amorphous Sugars

Figures 4.3.1 (a) show the water sorption isotherms of amorphous α-maltose (a-i), palatinose (a-ii), and trehalose (a-iii), prepared under different conditions. As shown in Fig. 4.3.1 (a-i), markedly less water sorption is observed for the vacuum-foam-dried α-maltose sample than for the aqueous freeze-dried sample, and no significant difference between the cases of using methanol or ethanol were found. The spray dried α-maltose samples show approximately the same amounts of sorbed water at given RHs as the aqueous freeze-dried sample, irrespective of the T_{inlet} (60˚C or 180˚C) (Fig. 4.3.1 (a-i)). In the case of palatinose (Fig. 4.3.1 (a-ii)), no significant difference in the water sorption isotherm between the different drying methods, nor between the different solvents used for vacuum foam drying were found. Fig. 4.3.1 (a-iii) shows less water sorption for the vacuum-foam-dried amorphous trehalose than that of the aqueous freeze-dried sample, the trend for which is similar to that for α-maltose (Fig. 4.3.1 (a-i)).

We assume that the free sugar hydroxyl groups in an amorphous sugar matrix serve as water sorption sites (Imamura et al., 2012; Kagotani et al., 2013) and can be qualitatively estimated for intensity of the IR absorption band due to the O-H stretching vibration for the sugar (Imamura et al., 2006; Kagotani et al., 2013). In actual fact, the amorphous α-maltose samples, that were vacuum-foam-dried from methanol and ethanol, exhibited ~21 cm^{-1} and ~16 cm^{-1} lower $\nu_{O\text{-}H}$ values, respectively, than the corresponding bands for the aqueous freeze-dried sample (Table 4.3.1), and their water sorption are the lowest and second lowest, respectively (Fig. 4.3.1 (a-i)). In the case of trehalose, the methanol-vacuum-foam-dried sample also shows markedly lower $\nu_{O\text{-}H}$ value and lower water than the aqueous freeze-dried sample (Fig. 4.3.1 (a-iii)). On the other hand, the amorphous α-maltose samples that had been spray-dried from methanol, contained nearly the same amounts of sorbed water (Fig. 4.3.1 (a-i)) as, but 12~14 cm^{-1} lower $\nu_{O\text{-}H}$ values (Table 4.3.1) than the aqueous freeze-dried one. A similar contradiction is observed for all the amorphous palatinose samples (Fig. 4.3.1 (a-ii)).

One possible explanation for the contradiction is that, similarly to the above-mentioned molecular agitation due to heating (Takeda et al., 2019), the sorption of water may function to relax the high molecular packing of the amorphous sugar matrix originated from being dried from alcohol. The combination of the water sorption as well as the heating during spray-drying may result in nearly the same water sorption for the spray-dried α-maltose as that of an aqueous freeze-dried sample (Fig. 4.3.1 (a-i)). On the other hand, in the case of palatinose, the IR spectra for the methanol- and ethanol-originated amorphous samples show stronger IR absorption due to >C=O stretching vibrations at around 1720 cm^{-1} compared to that of freeze-dried amorphous palatinose, indicating the formation of additional free carbonyl groups (probably originated from the ring opening of the fructopyranose moieties). A carbonyl group would have a greater affinity for water molecules than a sugar hydroxyl group. Consequently, the water sorption of the amorphous palatinose matrix, (vacuum-foam-) dried from alcohol, may possibly be increased to the level of those of the spray-dried and freeze-dried ones, by the increased water affinity of the matrix due to the increased carbonyl groups, as shown in Fig. 4.3.1 (a-ii).

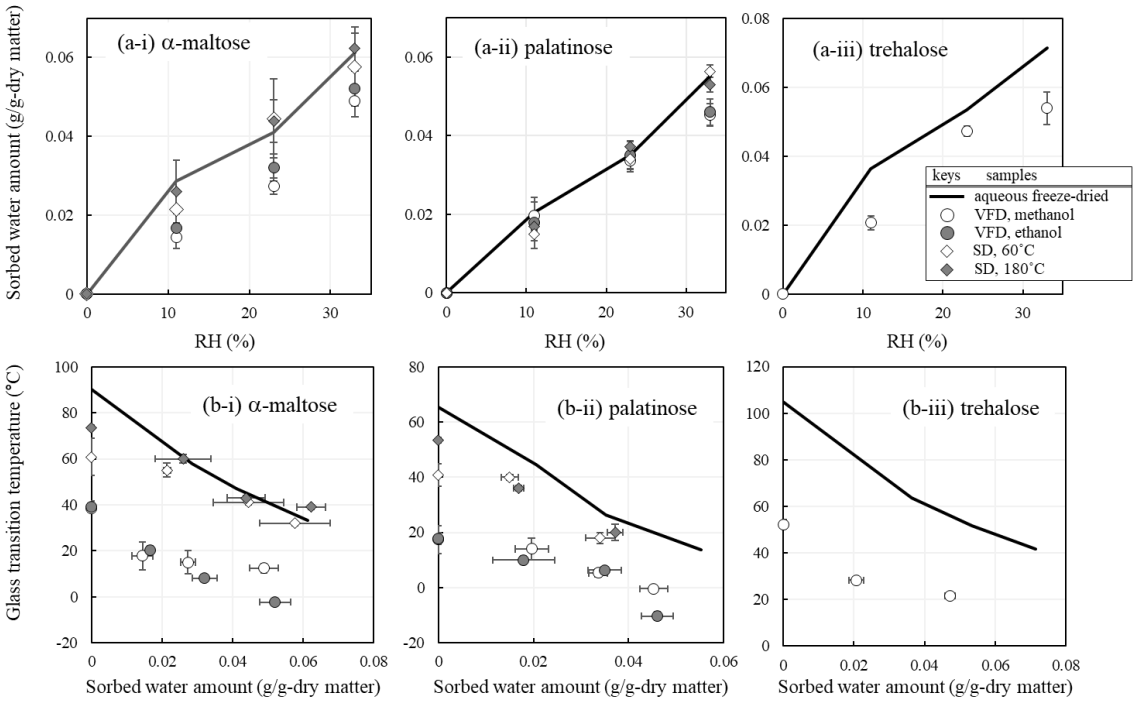

Fig. 4.3.1. (a) Water sorption isotherms of amorphous sugar matrices, dried under different conditions, and (b) their relationships with glass transition temperatures, T_g. The data are presented as mean ± deviation.

4.3.3. Dependence of the Glass Transition Temperature of Alcohol-Originated Amorphous Sugar on the Amount of Sorbed Water

The T_g values of the amorphous sugar samples that had been thoroughly dried and then moistened at given RHs, were determined and the values are shown as a function of the corresponding amount of sorbed water, in Figs. 4.3.1 (b). The T_g values of all the prepared samples tended to be decreased with increasing amount of sorbed water, which is due to the plasticizing effect of sorbed water (Roos & Karel, 1991b). Regarding vacuum-foam-drying, irrespective of the solvent type (methanol or ethanol), the curves for the relationship between T_g and amount of sorbed water lie, respectively, below those for the aqueous freeze-dried samples, as shown in Figs. 4.3.1 (b-i~iii). It should be noted that the difference in T_g between the vacuum-foam-dried and the aqueous freeze-dried sugars is generally around 50˚C in the thoroughly dried state and become smaller with increasing amount of sorbed water(Figs. 4.3.1 (b-i~iii)).

In comparing the data sets for the T_g and $\nu_{O\text{-}H}$ values for each tested sugar, it can be seen that the amorphous sugar sample, having higher $\nu_{O\text{-}H}$ value, tends to show a higher T_g value in the thoroughly dried state. Such a correlation was also observed in our previous studies (Sekitoh et al., 2021b) and was explained based on the molecular packing state of the prepared amorphous sugar samples (Sekitoh et al., 2021b). Namely, the greater extent of intermolecular hydrogen bonds, as indicated by the lower $\nu_{O\text{-}H}$ value, suggests higher molecular packing of the amorphous sugar matrix and inevitably therefore, a smaller space allocated to each sugar molecule. As the allocated volume for each sugar molecule in the amorphous matrix is smaller, a lower temperature would allow the actual molecular volume of sugar to expand beyond the allocated volume, resulting in a markedly low T_g value of the alcohol-vacuum-foam-dried amorphous sugar samples when the amount of sorbed water is zero (Figs. 4.3.1 (b-i~iii)).

As described above, the water sorption of amorphous sugar matrix appears to induce the relaxation of the high molecular packing of the amorphous sugar matrix, which would be naturally accompanied by an increase in the volume assigned to each sugar molecule in the amorphous matrix. Accordingly, the water sorption of the alcohol-originated amorphous sugar is considered to serve to shift (raise) the T_g value toward that of the aqueous freeze-dried sample. Consequently, the difference in T_g between the alcohol-vacuum-foam-dried and aqueous freeze-dried samples decreases with increasing RH, as

shown in Figs. 4.3.1 (b-i~iii).

The spray dried amorphous sugar (α-maltose, palatinose) samples show T_g values closer to those of the aqueous freeze-dried amorphous sugars in the thoroughly dried state, relative to that for the vacuum foam dried samples (Figs. 4.3.1 (b-i,ii)). The T_g values for T_{inlet} of 180˚C were ~10˚C higher than those for T_{inlet} of 60˚C in the thoroughly dried state. However, the T_g values for different T_{inlet} values (60˚C, 180˚C) coincide with each other when the amount of sorbed water is around 0.02 g/g-dry matter and then approaches those of the aqueous freeze-dried samples at amounts of sorbed water ≥ 0.02 g/g-dry matter (Figs. 4.3.1 (b-i, ii)).

As described above, the spray-drying that accompanies heating would relax the molecular packing of the methanol-originated amorphous sugar matrix. This would be the reason why spray-drying results in higher T_g values compared to vacuum-foam-drying as well as the reason for the higher T_g for higher T_{inlet}. In addition to this, further relaxation of the molecular packing of an amorphous sugar may be induced as the result of water sorption, as described above. As a result, the T_g values of the amorphous sugar samples that had been spray-dried at different T_{inlet} (60˚C, 180˚C), is assumed to coincide with each other for the amount of sorbed water of approximately 0.02 g/g-dry matter and then approach that of the water-originated samples with a further increase in the amount of sorbed water, as shown in Figs. 4.3.1 (b-i, ii).

Table 4.3.1 also shows a comparison of heat capacity shifts due to a glass-to-rubber transition (ΔC_p) for the amorphous sugar samples. The results suggest that the ΔC_p values for the vacuum foam dried and spray dried samples are generally the smallest and largest, respectively, of those for the three different drying methods.

When it is assumed that the C_p value of the sugar rubbery state (namely, at $>T_g$) is constant for each sugar, irrespective of the preparation conditions, it follows that a higher ΔC_p means a lower C_p value of the glassy state (at $<T_g$). The C_p value of a material is, in principle, reduced with increasing thermal mobility of the constituent molecules, whereas the thermal molecular mobility of an amorphous sugar matrix may be more restricted by a greater extent of hydrogen bonding between the sugar molecules. Consequently, judging from the $\nu_{O\text{-}H}$ values (Table 4.3.1), the spray dried and vacuum foam dried samples would be expected to have lower C_p of the glassy state and thus exhibit greater ΔC_p values than the aqueous freeze-dried samples. These considerations

coincide with the comparatively high ΔC_p values of the spray dried samples (Table 4.3.1) but appear to conflict with the lowest ΔC_p values of the vacuum-foam-dried samples (Table 4.3.1). The discordance concerning the ΔC_p of the vacuum-foam-dried samples can possibly be explained as follows: The high molecular packing of an amorphous sugar that is vacuum-foam-dried from alcohol, may also be relaxed by the upward temperature scan during the DSC measurement. The additional energy, associated with the relaxation of the packing in the case of the amorphous sugar matrix, may increase the C_p of the glassy state (at $<T_g$) and consequently lower the ΔC_p value, as shown in Table 4.3.1.

4.4. Conclusions

Amorphous sugar (α-maltose, palatinose, trehalose) matrices were prepared under different processing conditions, namely, freeze-drying from water, vacuum-foam-drying from alcohols (methanol, ethanol), and spray-drying from methanol. The differently prepared amorphous sugar samples were compared for their water sorption isotherm and the dependence of the glass transition temperature (T_g) on the amount of sorbed water. The hydrogen bonding states of the dried amorphous sugar matrices and the partial molar volumes of sugars in methanol as well as water were also analyzed. The results revealed that a sugar molecule has a more compact conformation in methanol than in water. Such a compact conformation of a sugar molecule in alcohol is considered to be non-negligibly carried over in the amorphous sugar matrix, when vacuum foam dried that is not accompanied by heat. It may follow that the molecular packing of the amorphous sugar matrix is strengthened, followed by the increased intermolecular hydrogen bonding between sugar molecules, in other words, the decreased free hydroxyl groups in the matrix. As a result, the alcohol vacuum-foam-dried amorphous sugar may exhibit lower T_g and contain less sorbed water, respectively, than the corresponding aqueous freeze-dried sample. On the other hand, since spray-drying is inevitably associated with heating of the dried particles, the molecular packing state of the alcohol-originated amorphous sugar would be relaxed to some extent through the spray-drying process. As a result, the methanol spray-dried amorphous sugar appears to exhibit T_g and water sorption values that are closer to those of the aqueous freeze-dried sample, compared to the alcohol vacuum-foam-dried sample. The differences in T_g between the aqueous freeze-dried and the alcohol-originated (vacuum-foam- or spray-dried) amorphous sugars

appeared to decrease with increasing amount of sorbed water. This suggests that water sorption also may serve to relax the molecular packing of the alcohol-originated amorphous sugar matrix, similarly to heating during spray-drying. However, the water sorption isotherms of the amorphous palatinose samples that were prepared under different conditions, were quite consistent with each other. This can be attributed to the specific nature of palatinose, namely, the formation of carbonyl groups through the opening of the fructopyranose ring during drying from alcohol.

Chapter 5 Conclusions and Remarks on the Future Study

5.1. Conclusions

This thesis was dedicated to (I) applying a novel sugar amorphization technique, based on the over-dissolution of sugar in alcohol, to a solid dispersion of poorly water-soluble drugs and (II) understanding the impact of preparation procedures (solvent type, drying method and condition, etc) on the physicochemical properties of the alcohol-originated amorphous sugar. The following conclusions were obtained from this study.

Chapter 2

In this chapter, a Sole-Amorphous-Sugar-based Solid Dispersion (SAS-SD), with hydrophobic model drugs embedded in them, were prepared and evaluated for its effectiveness in improving the model drug solubility in water. Actual SAS-SD procedure was as follows: A freeze-dried amorphous sugar sample was dissolved in an organic solvent, that contained a soluble model hydrophobic component; The suspension of the sugar and the model hydrophobic component was vacuum foam dried to give a solid powder. Four types of sugars and methanol were used as representative sugars and the organic medium. Four model drugs (indomethacin, ibuprofen, gliclazide, and nifedipine) were employed. A DSC analysis indicated that the sugar and model drug did not undergo segregation during the drying process. The dissolution of the hydrophobic drugs in water from the solid dispersion was then evaluated, and the results indicated that the initial dissolution of the hydrophobic drug in water was increased when the SAS-SD was used. Palatinose and/or α-maltose were superior to the other tested carbohydrates in increasing the initial dissolution for all tested model drugs, and the model drug with a lower water solubility tended to exhibit a greater extent of over dissolution.

Chapter 3

An amorphous sugar matrix, which was dried from an organic solvent, was investigated for use as method for dispersing hydrophobic drugs. However, the amorphous sugar, originally contained in the organic solvent, exhibited significantly low glass transition

temperature (T_g) and thus has physically unstable. This chapter examined the physicochemical properties of a sugar in a dried matrix and in an organic solvent, using α-maltose and methanol as a representative sugar and organic solvent. The apparent molar volume of α-maltose was ~30% smaller in methanol than in water. The methanol-originated amorphous α-maltose exhibited much greater degree of hydrogen bonding than the water-originated one. Considering these findings, it was concluded that the compact conformation of α-maltose persisted in the dried state and consequently caused the markedly low T_g. Secondly, it was found that heating under appropriate conditions resulted in an increase in the T_g of the methanol-originated amorphous α-maltose as well as a decrease in the level of hydrogen bonding. The aqueous dissolution of two model hydrophobic drugs (indomethacin and ibuprofen) from the surfactant-free solid dispersion were also improved as the result of the heat-treatment, while, to the contrary, the dissolution of another model drug (curcumin) was lowered.

Chapter 4

This Chapter aimed to understand the impact of preparation conditions on the physicochemical characteristics of amorphous sugar. Amorphous sugar (α-maltose, isomaltulose, trehalose) matrices were prepared from alcohol solutions (methanol, ethanol), and their water sorption behavior and glass transition temperatures, T_g, were compared with those of aqueous freeze-dried amorphous sugar. Vacuum-foam- and spray-drying procedures were employed as drying methods. Water sorption for amorphous sugars, dried by different methods, was generally significant in the following order: vacuum-foam-drying< spray-drying≤ freeze-drying. In the same order, the T_g values for the thoroughly dried amorphous sugars increased, and water sorption appeared to reduce the differences in T_g for given amounts of sorbed water. The solvent type used in vacuum-foam-drying slightly affected the water sorption as well as the dependence of T_g on the sorbed water amount. The inlet temperature of hot air used in the spray-drying slightly influenced the T_g in the thoroughly dried state. These tendencies are discussed based on the molecular packing of amorphous sugar matrices. The obtained findings suggested that physicochemical characteristics of amorphous sugar may depend on the sugar molecule conformation in solvent and dried state.

5.2. Remarks on the Future Study

This thesis demonstrated that the SAS-SD technique successfully improved the aqueous dissolution of hydrophobic drugs. Although the SAS-SD samples exhibited markedly poor physicochemical stability, represented by the markedly low T_g value, the instability of the alcohol-originated amorphous sugar also could be improved by adequate thermal annealing (treatment). Accordingly, the SAS-SD technique can be concluded to be promising as an alternative one to increase the bioavailability of hydrophobic drugs. However, there remains a drawback to this novel solid dispersion technique. That is, when the content of the hydrophobic drug in the SAS-SD formulation increases above a certain ratio, the segregation of the drug from the amorphous sugar phase becomes significant, resulting in the crystallization. According to this restriction, the content of the hydrophobic drug in the SAS-SD formulation was limited to 1 wt% in this study.

On the other hand, considering the finding that the T_g of the SAS-SD and the aqueous dissolution of the drug from the SAS-SD samples were markedly increased by the thermal annealing, a spray-drying appeared superior to a vacuum foam one. Actually, the T_g value of the amorphous sugar, spray-dried (from alcohol), was higher than that of the vacuum-foam-dried one. However, the usage of spray-drying encountered another problem that the crystallization of sugar and hydrophobic drug became more significant than in the case of vacuum-foam-drying.

Considering these, it would be the next focus of the study to establish the methodology to increase the content of hydrophobic drug in the SAS-SD formulation, keeping the drug component uniformly dispersed. If the further study enables the sufficient incorporation of hydrophobic drugs in the alcohol-originated amorphous sugar, I hope, the SAS-SD may possibly bring innovation to a drug delivery technique.

Reference

Aceves, J. M., Cruz, R., Hernandez, E., 2000. Preparation and characterization of Furosemide-Eudragit controlled release systems. *Int. J. Pharm.* 195 (1-2), 45-53.

Ahuja, G., Pathak, K., 2009. Porous carriers for controlled/modulated drug delivery. *Indian J. Pharm. Sci.* 71 (6), 599-607.

Alkilany, A. M., Abulateefeh, S. R., Mills, K. K., Bani Yaseen, A. I., Hamaly, M. A., Alkhatib, H. A., Aiedeh, K. M.; Stone, J. W. 2014. Colloidal stability of citrate and mercaptoacetic acid capped gold nanoparticles upon lyophilization: Effect of capping ligand attachment and type of cryoprotectants. *Langmuir* 30(46), 13799-13808.

Amidon, G. L., 1991. Drug derivatization as a means of solubilizations: Physical and biochemical strategies. In: Yalkowsky SH., eds. *Techniques of Solubilization of Drug*. New York: Marcel Dekker, p 183-211.

Amidon, G. L., Lennernas, H., Shah, V. P., Crison, J. R., 1995. A theoretical basis for a biopharmaceutic drug classification: The correlation of *in vitro* drug product dissolution and *in vivo* bioavailability. *Pharm*. *Res*. 12, 413-420.

Arevalo-Pinedo, A., Murr, F., 2006. Kinetics of vacuum drying of pumpkin (Cucurbita maxima): Modeling with shrinkage. *J. Food Eng.* 76(4), 562–567.

Banerjee, P., Amidon, G., 1985. Design of prodrugs based on enzymes-substrate specificity. In: Bundgaard H, eds. *Design of Prodrugs.*, New York: Elsevier, p 93-133.

Banipal, P. K., Banipal, T. S., Lark, B. S., Ahluwalia, J. C., 1997. Partial molar heat capacities and volumes of some mono-, di- and tri- saccharides in water at 298.15, 308.15 and 318.15 K. *J. Chem. Soc. Faraday Trans.* 93, 81-87.

Benita, S., Levy, M. Y., 1993. Submicron emulsions as colloidal drug carriers for intravenous administration: Comprehensive physicochemical characterization. *J. Pharm. Sci.* 82 (11), 1069-1079.

Bevilacqua, A., Costa, C., Corbo, M. R., Sinigaglia, M., 2009. Effects of the high pressure of homogenization on some spoiling micro-organisms, representative of fruit juice microflora, inoculated in saline solution. *Lett. Appl. Microbiol.* 48 (2), 261-267.

Bhandari, B. R., Hartel, R. W., 2005. Phase transition during food powder production and powder stability. In: Onwulata C, Konstance RP, eds., *Encapsulated and Food Powder;* New York, Marcel Dekker, pp. 261-292.

Bogdanova, E., Fureby, A. M., Kocherbitov, V., 2021. Hydration enthalpies of amorphous sucrose, trehalose and maltodextrins and their relationship with heat capacities. *Phys. Chem. Chem. Phys.*, 23(26), 14433-14448.

Brouwers, J., Brewster, M. E., Augustijns, P., 2009. Supersaturating drug delivery systems: the answer to solubility-limited oral bioavailability? *J. Pharm. Sci*. 98, 2549–2572.

Buera, P., Schebor, C., Elizalde, B., 2005. Effect of carbohydrate crystallization on stability of dehydrated foods and ingredient formulations. *J. Food Eng.* 67(1-2), 157-165.

Carolina, B. C., Carolina, S., Zamora, M., Jorge, C., 2007. Glass transition temperatures and some physical and sensory changes in stored spray-dried encapsulated flavors. *LWT* 40, 1792-1797.

Carpenter, J. F., Prestrelski, S. J., Anchordoguy, T. J., Arakawa, T., 1994. Interactions of proteins with stabilizers during freezing and drying. In: Cleland JL, Langer R, eds. Formulation and delivery of proteins and peptides. Washington, DC: *ACS Symposium Series*, Vol. 567, p 134-147.

Cassanelli, M., Norton, I ., Mills, T., 2018. Interaction of mannitol and sucrose with gellan gum in freeze-dried gel systems. *Food Biophys.* 13(3), 304-315.

Chadha, R., Kapoor, V. K., Kumar, A., 2006. Analytical techniques used to characterize drug-polyvinylpyrrolidone systems in solid and liquid states - An overview. *J. Sci. Ind. Res*. 65, 459-469.

Chang, B. S., Beauvais, R. M., Dong, A., Carpenter, J. F., 1996. Physical factors affecting the storage stability of freeze-dried interleukin-1 receptor antagonist: glass transition and protein conformation. *Arch. Biochem. Biophys.* 331, 249-258.

Chang, H. I., Yeh, M. K., 2012, Clinical development of liposome-based drugs: Formulation, characterization, and therapeutic efficacy. *Int. J. Nanomedicine* 7, 49-60.

Chen, X. D., 2007. Conformability of the kinetics of cohesion/stickiness development in amorphous sugar particles to the classical Arrhenius law. *J. Food Eng.* 79(2), 675-680.

Cho, C. S., Shin, T. H., Lim, J. L., Moon, K. Y., Kim, D. K., Choi, Y. W., 2010. Stability-enhanced solid dispersion formulation of amorphous raloxifene hydrochloride. *Korean J. Chem. Eng.* 27 (6), 1906-1909.

Cho, Y., Ha, E. S., Baek, I. H., Kim, M. S., Cho, C. W., Hwang, S. J., 2015 Enhanced supersaturation and oral absorption of sirolimus using an amorphous solid dispersion

based on Eudragit® E. *Molecules* 20 (6), 9496-9509.

Crowe, J. H., Crowe, L. M., Chapman, D., 1984. Preservation of membranes in anhydrobiotic organisms – The role of trehalose. *Science* 223, 701-703.

Crowe, J. H., Crowe, L. M., Carpenter, J. F., Wistrom, C. A., 1987. Stabilization of dry phospholipid bilayers and proteins by sugars. *Biochem. J.* 242, 1-10.

Desai, K. G. H., Park, H. J., 2005. Recent developments in microencapsulation of food ingredients. *Dry. Technol.* 23, 1361-1394.

van Drooge, D. I., Hinrichs, W. L. J., Frijlink, H. W., 2004. Incorporation of lipophilic drugs in sugar glasses by lyophilization using a mixture of water and tertiary butyl alcohol as solvent. *J. Pharm. Sci.*, 93(3), 713-725.

van Eerdenbrugh, B., van den Mooter, G., Augustijns, P., 2008. Top-down production of drug nanocrystals: nanosuspension stabilization, miniaturization and transformation into solid products. *Int. J. Pharm.* 364 (1), 64-75.

Fan, W., Zhang, X., Zhu, W., Di, L., 2020. The preparation of curcumin sustained-release solid dispersion by hot-melt extrusion- Ⅱ. Optimization of preparation process and evaluation *in vitro* and *in vivo*. *J. Pharm. Sci.* 109 (3), 1253-1260.

Flores, M. V., Naraghi, K., Engasser, J-M., Halling, P. J., 2002. Influence of glucose solubility and dissolution rate on the kinetics of lipase catalyzed synthesis of glucose laurate in 2-methyl 2-butanol. *Biotechnol. Bioeng*. 78, 815–821.

Fox, T. G., Flory, P. J., 1950. Second-order transition temperatures and related properties of polystyrene. I. Influence of molecular weight. *J. Appl. Phys.* 21, 581–591.

Franks, F., Hatley, R. H. M., Mathias, S. F., 1991. Materials science and the production of shelf-stable biologicals. *Biopharm-Technol. Bus*. 4 (9), 38-42.

Fujioka, A., Yamamoto, R., Tramis, O., Ishida, H., Ono, T., Ishida, N., Imamura, K., 2022. Induction of foaming in vacuum drying by needle stimulation and the impact of solution viscosity, vapor pressure, and the type of solute and solvent. *Dry. Technol.* 40(15), 3249-3261.

Gao, P., Shi, Y., 2012. Characterization of supersaturatable formulations for improved absorption of poorly soluble drugs. *AAPS J.* 14, 703-713.

Gharsallaoui, A., Roudaut, G., Chambin, O., Voilley, A., Saurel, R., 2007. Applications of spray-drying in microencapsulation of food ingredients: an overview. *Food Res. Int.* 40, 1107-1121.

Greenspan, L., 1977. Humidity fixed points of binary saturated aqueous solutions. *J. Res. Nat. Bur. Stand. A Phys. Chem.* 81(1), 89-96.

Ha, E. S., Choo, G. H., Baek, I. H., Kim, M. S., 2014. Formulation, characterization, and *in vivo* evaluation of celecoxib-PVP solid dispersion nanoparticles using supercritical antisolvent process. *Molecules* 19 (12), 20325-20339.

Hancock, B. C., Zografi, G., 1997. Characteristics and significance of the amorphous state in pharmaceutical system. *J. Pharm. Sci.* 86, 1-12.

Hancock, B. C., Shamblin, S. L., 1998. Water vapour sorption by pharmaceutical sugars. *Pharm. Sci. Technol. Today* 1, 345-351.

Hancock, B. C., Dalton, C. R., 1999. The effect of temperature on water vapor sorption by some amorphous pharmaceutical sugars. *Pharm. Dev. Technol.* 4(1), 125-131.

Hancock, B., Parks, M., 2000. What is the true solubility advantage for amorphous pharmaceuticals? *Pharm. Res*. 17, 397–404.

Harnkarnsujarit, N., Charoenrein, S., 2011. Effect of water activity on sugar crystallization and ß-carotene stability of freeze-dried mango powder. *J. Food Eng.* 105 (4), 592-598.

Hartel, R. W., Shastry, A. V., 1991. Sugar crystallization in food products. *Crit. Rev. Food Sci. Nutr.* 30, 49–112.

Heljo, V. P., Nordberg, A., Tenho, M., Virtanen, T., Jouppila, K., Salonen, J., Maunu, S. L., Juppo, A. M., 2012. The effect of water plasticization on the molecular mobility and crystallization tendency of amorphous disaccharides. *Pharm. Res.* 29(10), 2684-2697.

Hidaka, F., Sato, T., Fujioka, A., Takeda, K., Imanaka, H., Ishida, N., Imamura, K., 2018. Controlling the drying process in vacuum foam drying under low vacuum conditions by inducing foaming by needle stimulation of the solution. *Dry. Technol.* 37 (12), 1520-1527.

Hilden, L. R. L., Morris, K. R. K., 2003. Physics of amorphous solids. *J. Pharm. Sci.* 93, 3-12.

Huang, Y., Dai, W. G., 2014. Fundamental aspects of solid dispersion technology for poorly soluble drugs. *Acta Pharm. Sinica B* 4, 18-25.

Ilevbare, G. A., Liu, H., Edgar, K. J., Taylor, L. S., 2013. Maintaining supersaturation in aqueous drug solutions: impact of different polymers on induction times. *Cryst. Growth Design* 13, 740-751.

Imamura, K., Iwai, M., Ogawa, T., Sakiyama, T.; Nakanishi, K., 2001. Evaluation of

hydration states of protein in freeze-dried amorphous sugar matrix. *J. Pharm. Sci.* 90, 1955–1963.

Imamura, K., Sakaura, K., Ohyama, K., Fukushima, A., Imanaka, H., Sakiyama, T., Nakanishi, K., 2006. Temperature scanning FTIR analysis of hydrogen bonding states of various saccharides in amorphous matrixes below and above their glass transition temperatures. *J. Phys. Chem. B* 110, 15094-15099.

Imamura, K., Asano, Y., Maruyama, Y., Yokoyama, T., Nomura, M., Ogawa, S., Nakanishi, K., 2008. Characteristics of hydrogen bond formation between sugar and polymer in freeze-dried mixtures under different rehumidification conditions and its impact on the glass transition temperature. *J. Pharm. Sci.* 97, 1301-1312.

Imamura, K., Maruyama, Y., Tanaka, K., Yokoyama, T., Imanaka, H., Nakanishi, K., 2008. True density analysis of a freeze-dried amorphous sugar matrix. *J. Pharm. Sci.* 97, 2789–2797.

Imamura, K., Ohyama, K., Yokoyama, T., Maruyama, Y., Nakanishi, K., 2009. Temperature scanning FTIR analysis of secondary structures of proteins embedded in amorphous sugar matrix. *J. Pharm. Sci.* 98, 3088–3098.

Imamura, K., Yokoyama, T., Fukushima, A., Kinuhata, M., Nakanishi, K., 2010a. Water sorption, glass transition, and protein-stabilizing behavior of an amorphous sucrose matrix combined with various materials. *J. Pharm. Sci*. 99, 4669-4677.

Imamura K, Nomura M, Tanaka K, Kataoka N, Oshitani J,Imanaka H, Nakanishi, K. 2010b. Impacts of compression on crystallization behavior of freeze-dried amorphous sucrose. *J. Pharm. Sci.* 99, 1452–1463.

Imamura, K., Kagotani, R., Nomura, M., Kinugawa, K., Nakanishi, K., 2012. Heterogeneity of the state and functionality of water molecules sorbed in an amorphous sugar matrix. *Carbohydr. Res.* 351, 108-113.

Imamura, K., Ishida, N., Imanaka, H., Satoh, T., Miyake, K., Yoshiyama, N., Matsuura, T., 2014. Japanese pantent application No. 2014-06195.

Jang, D. J., Kim, S. T., Lee, K., Oh, E., 2014. Improved bioavailability and antiasthmatic efficacy of poorly soluble curcumin-solid dispersion granules obtained using fluid bed granulation. *BioMed. Mater. and Eng.* 24, 413-429.

Jayne, L. M., Rees, G. D., 2000. Micro-emulsion-based media as novel drug delivery systems. *Adv. Drug Delivery Rev*. 45, 89-121.

Jie, L., Jianming, C., Yi, L., Jing, S., Fuqiang, H., Zongning, Y., Wei, W., 2009. Glyceryl monooleate/Poloxamer 407 cubic nanoparticles as oral drug delivery Systems: I. *In vitro* evaluation and enhanced oral bioavailability of the poorly water-soluble drug simvastatin. *AAPS PharmSciTech* 10, 960-966.

Jonsdottir, R., Bragadottir, M., Örn, A. G., 2005. Oxidatively derived volatile compounds in microencapsulated fish oil monitored by solid-phase microextraction (SPME). *J. Food Sci.* 70, C433-440.

Jouppila, K., Roos, Y. H., 1994. Glass transitions and crystallization in milk powders. *J. Dairy Sci.* 77(10), 2907-2915.

Kagotani, R., Kinugawa, K., Nomura, M., Imanaka, H., Ishida, N., Imamura, K., 2013. Improving the physical stability of freeze-dried amorphous sugar matrices by compression at several hundreds MPa. *J. Pharm. Sci.* 102, 2187-2197.

Kasim, N. A., Whitehouse, M., Ramachandran, C., Bermejo, M., Lennernas, H., Hussain, A. S., Junginger, H. E., Stavchansky, S. A., Midha, K. K., Shah, V. P., Amidon, G. L., 2004. Molecular properties of WHO essential drugs and provisional biopharmaceutical classification. *Mol. Pharm*. 1, 85–96.

Kedward, C. J., MacNaughtan, W., Mitchell, J. R., 1998. Isothermal and non-isothermal crystallization in amorphous sucrose and lactose at low moisture contents. *J. Food Sci.* 63, 192–197.

Kedward, C. J., MacNaughtan, W., Mitchell, J. R. 2000a. Crystallization kinetics of amorphous lactose as a function of moisture content using isothermal differential scanning calorimetry. *J. Food Sci.* 65(2), 324-328.

Kedward, C. J., MacNaughtan, W., Blanshard, J. M. V., Mitchell, J. R., 2000b. Crystallization kinetics of lactose and sucrose based on isothermal differential scanning calorimetry. *Carbohydr. Res.* 329, 423–430.

Kennedy, M., Hu, J., Gao, P., Li, L., Ali-Reynolds, A., Chal, B., Gupta, V., Ma, C., Mahajan, N., Akrami, A., Surapaneni, S., 2008. Enhanced bioavailability of a poorly soluble VR1 antagonist using an amorphous solid dispersion approach: a case study. *Mol. Pharm.* 5 (6), 981-993.

Kesisoglou, F., Panmai, S., Wu, Y., 2007. Nanosizing-oral formulation development and biopharmaceutical evaluation. *Adv. Drug Deliv. Rev.* 59 (7), 631-644.

Kinugawa, K., Kinuhata, M., Kagotani, R., Imanaka, H., Ishida, N., Kitamatsu, M., Nakanishi, K., Imamura, K., 2015. Inhibitory effects of additives and heat treatment on the crystallization of freeze-dried sugar. *J. Food Eng.* 155, 37–44.

Kuang, P. Q., Zhang, H. C., Bajaj, P. R., Yuan, Q. P., Tang, J. M., Chen, S. L., Sablani, S. S., 2015, Physicochemical properties and storage stability of lutein microcapsules prepared with maltodextrins and sucrose by spray drying. *J. Food Sci.* 80(2), E359-E369.

Lai, J., Chen, J., Lu, Y., Sun, J., Hu, F., Yin, Z., Wu, W., 2009. Glyceryl monooleate/poloxamer 407 cubic nanoparticles as oral drug delivery systems: I. *In vitro* evaluation and enhanced oral bioavailability of the poorly water-soluble drug simvastatin. *AAPS PharmSciTech* 10 (3), 960-966.

Lavra, Z. M., Pereira de Santana, D., Ré, M. I., 2017. Solubility and dissolution performances of spray-dried solid dispersion of Efavirenz in Soluplus. *Drug Dev. Ind. Pharm.* 43 (1), 42-54.

Leuner, C., Dressman, J., 2000. Improving drug solubility for oral delivery using solid dispersions. *Eur. J. Pharm. Biopharm.* 50, 47-60.

Li, B., Konecke, S., Harich, K., Wegiel, L., Taylor, L. S., Edgar, K. J., 2013. Solid dispersion of quercetin in cellulose derivative matrices influences both solubility and stability. *Carbohydr. Polym*. 92, 2033–2040.

Li, W., Yun, L. Y., Zhao, Y. J., Zhi, Z. J., Muhindo, E. M., Geng, X. Y., Liu, R., Wu, T., Sui, W. J., Zhang, M., 2022. Effect of water sorption on glass transition and microstructural variation of dextran and sugar mixtures. *Carbohydr. Polym.* 290, 119505.

Li, Y. P., Zhang, X. Y., Zhou, J. J., Pei, Y. Y., 1999. Preparation and dissolution property of ipriflavone solid dispersion. *Zhongguo Yao Li Xue Bao* 20 (10), 957-960.

Li, Z., Barnes, J. C., Bosoy, A., Stoddart, J. F., Zink, J. I., 2013. Mesoporous silica nanoparticles in biomedical applications. *Chem. Soc. Rev.* 41, 2590–2605.

Lin, S-Y., 1992. Isolation and solid-state characteristics of a new crystal form of indomethacin. *J. Pharm. Sci*. 81, 572-576.

Lipinski, C. A., 2002. Poor aqueous solubility-an industry wide problem in drug discovery. *Am. Pharm. Rev*. 5, 82-85.

Liu, C., Chen, Z., Chen, Y., Lu, J., Li, Y., Wang, S., Wu, G., Qian, F., 2016. Improving oral bioavailability of sorafenib by optimizing the “spring” and “parachute” based on molecular interaction mechanisms. *Mol. Pharm.* 13, 599-608.

Liu, Y. T., Bhandari, B., Zhou, W. B., 2006. Glass transition and enthalpy relaxation of amorphous food saccharides: A review. *J. Agric. Food Chem*. 54, 5701-5717.

Liu, W. R., Langer, R., Klibanov, A. M., 1991. Moisture-induced aggregation of lyophilized proteins in the solid state. *Biotechnol. Bioeng.* 37 (2), 177-184.

Lloyd, G. R., Craig, D. Q., Smith, A., 1997. An investigation into the melting behavior of binary mixes and solid dispersions of paracetamol and PEG 4000. *J. Pharm. Sci*. 86, 991-996.

Löbenberg, R., Amidon, G. L., 2000. Modern bioavailability, bioequivalence and biopharmaceutics classification system. New scientific approach to international regulatory standards. *Eur. J. Pharm. Biopharm.* 50, 3–12.

Lopalco, A., Iacobazzi, R. M., Denora, N., Stella, V. J., 2021. Bortezomib aqueous solubility in the presence and absence of D-mannitol: A clarification with formulation implications. *J. Pharm. Sci.* 110 (1), 543-547.

Lust, A., Laidmäe, I., Palo, M., Meos, A., Aaltonen, J., Veski, P., Heinämäki, J., Kogermann, K., 2013. Solid-state dependent dissolution and oral bioavailability of piroxicam in rats. *Eur. J. Pharm. Sci.* 48 (1-2), 47-54.

Manning, M. C., Patel, K., & Borchardt, R.T. 1989. Stability of protein pharmaceuticals. *Pharm. Res.* 6, 903-918.

Marinaro, W. A., Schieber, L. J., Munson, E. J., Day, V. W., Stella, V. J., 2012. Properties of a model aryl boronic acid and its boroxine. *J. Pharm. Sci.* 101 (9), 3190-3198.

Matteucci, M. E., Paguio, J. C., Miller, M. A., 2009. Williams, R. O.; Johnson, K. P. Highly supersaturated solutions from dissolution of amorphous itraconazole microparticles at pH 6.8. *Mol. Pharm*. 6, 375–385.

Meng, F., Ferreira, R., Su, Y., Zhang, F., 2021. A novel amorphous solid dispersion based on drug-polymer complexation. *Drug Deliv. Transl. Res.* 11 (5), 2072-2084.

Miller, D. P., de Pablo, J. J., Corti, H. R., 1999. Viscosity and glass transition temperature of aqueous mixtures of trehalose with borax and sodium chloride. *J. Phys. Chem. B* 103, 10243–10249.

Modi, A., Tayade, P., 2006. Enhancement of dissolution profile by solid dispersion (kneading) technique. *AAPS PharmSciTech* 7 (3), 68.

Morteza, S., Amirali, E., Timothy, L. A., 2016. A novel formulation for solubility and content uniformity enhancement of poorly water-soluble drugs using highly-porous

mannitol. *Eur. J. Pharm. Sci*. 83, 52-61.
Mukesh, S., Joshi, P., Bansal, A. K., Kashyap, M. C., Mandal, S. K., Sathe, V., Sangamwar, A. T., 2021. Amorphous salts solid dispersions of celecoxib: Enhanced biopharmaceutical performance and physical stability. *Mol. Pharm.* 18 (6), 2334-2348.
Nagane, K., Kimura, S., Ukai, K., Ogawa, N., Yamamoto, H., 2014. Practical approach to prepare solid dispersion drug product using spherical silicate. *Int. J. Pharm.* 475 (1-2), 364-371.
Nguyen, T. N., Tran, P. H., Van Vo, T., Duan, W., 2016. Truong-Dinh Tran, T., Development of a sustained release solid dispersion using swellable polymer by melting method. *Pharm. Res.* 33 (1), 102-109.
Nie, H., Mo, H., Zhang, M., Song, Y., Fang, K., Taylor, S., Li, T., Byrn, 2015. S. R. Investigating the interaction pattern and structural elements of a drug-polymer complex at the molecular level. *Mol. Pharm*. 12, 2459-2468.
Nie, H., Su, Y., Zhang, M., Song, Y., Leone, A., Taylor, S., Marsac, P. J., Li, T., Byrn, S. R., 2016. Solid-state spectroscopic investigation of molecular interactions between Clofazimine and hydpromellose phthalate in amorphous solid dispersions. *Mol. Pharm*. 13, 3964-3975.
Ogawa, N., Hiramatsu, T., Suzuki, R., Okamoto, R., Shibagaki, K., Fujita, K., Takahashi, C., Kawashima, Y., Yamamoto, H., 2018. Improvement in the water solubility of drugs with a solid dispersion system by spray drying and hot-melt extrusion with using the amphiphilic polyvinyl caprolactam-polyvinyl acetate-polyethylene glycol graft copolymer and d-mannitol. *Eur. J. Pharm. Sci.* 111, 205-214.
Ohtake, S., Schebor, C., Palecek, S. P., de Pablo, J. J., 2004. Effect of pH, counter ion, and phosphate concentration on the glass transition temperature of freeze-dried sugar-phosphate mixtures. *Pharm. Res.* 21, 1615-1621.
Okamoto, T., Yamamoto, K., Sekitoh, T., Fujioka, A., Imanaka, H., Ishida, N., Imamura, K., 2022. Comparison of improvements of aqueous dissolution of structurally analogous hydrophobic drugs by amorphous solid dispersion. *Colloid Surf. A* 632, 127744.
Orford, P. D., Parker, R., Ring, S. G., 1990. Aspects of the glass transition behavior of mixtures of carbohydrates of low molecular weight. *Carbohydr. Res.* 196, 11-18.
Palomaki, E. A. K., Lipiainen, T., Strachan, C. J., Yliruusi, J. K., 2020. Effect of trehalose and melibiose on crystallization of amorphous paracetamol. *Int. J. Pharm.* 590, 119878.

Paramita, V., Iida, K., Yoshii, H., Furuta, T., 2010. Effect of feed liquid temperature on the structural morphologies of d-limonene microencapsulated powder and its preservation. *J. Food Sci.* 75 (1), E39-45.

Patil, H., Tiwari, R. V., Repka, M. A., 2016. Hot-melt extrusion: From theory to application in pharmaceutical formulation. *AAPS PharmSciTech* 17 (1), 20-42.

Pikal, M. J., 1994. Freeze-drying of proteins. Process, formulation and stability. In: Cleland, J. L., Langer, R., eds. Formulation and delivery of proteins and peptides, Washington, DC: *ACS Symposium Series*, Vol. 567, p 120-133.

Pisal, S., Wawde, G., Salvankar, S., Lade, S., Kadam, S., 2006. Vacuum foam drying for preservation of LaSota Virus: Effect of additves. *AAPS PharmSciTech*. 7, E1-E8.

Pokharkar, V. B., Leenata, P. M., Mahesh, N. P., Anshuman, A., Ambike, K. R. M., Anant, P., 2006. Development, characterization and stabilization of amorphous form of a low Tg drug. *Powder Technol.* 167, 20-25.

Porter, C. J. H., Charman, S. A., 1996. Williams, R. D.; Bakalova, M. V.; Charman, W. N. Evaluation of emulsifiable glasses for the oral administration of cyclosporin in beagle dogs. *Int. J. Pharm.* 141, 227-237.

Pouton, C. W., 1997. Formulation of self-microemulsifying delivery system. *Adv. Drug Delivery Rev*. 25, 47-58.

Prasad, R., Radhakrishnan, P., Singh, S. K., Verma, P. R. P., 2017. Furosemide - Soluplus® solid dispersion: Development and characterization. *Recent Pat. Drug Deliv. Formul.* 11 (3), 211-220.

Qi, S., Gryczke, A., Belton, P., Craig, D. Q., 2008. Characterisation of solid dispersions of paracetamol and Eudragit E prepared by hot-melt extrusion using thermal, microthermal and spectroscopic analysis. *Int. J. Pharm.* 354 (1-2), 158-167.

Rautio, J., Kumpulainen, H., Heimbach, T., Oliyai, R., Oh, D., Järvinen, T., Savolainen, J., 2008. Prodrugs: Design and clinical applications. *Nat. Rev. Drug Discov.* 7 (3), 255-270.

Repka, M. A., Shah, S., Lu, J., Maddineni, S., Morott, J., Patwardhan, K., Mohammed, N. N., 2012. Melt extrusion: Process to product. *Expert Opin. Drug Delive.* 9 (1), 105-125.

Roos, Y., Karel, M., 1990. Differential scanning calorimetry study of phase transitions affecting the quality of dehydrated materials. *Biotechnol. Progr.* 6, 159-163.

Roos, Y., Karel, M., 1991a. Water and molecular weight effects on glass transitions in amorphous carohydrates and carbohydrate solutions. *J. Food Sci*. 56, 1676-1681.

Roos, Y., Karel, M., 1991b. Plasticizing effect of water on thermal behavior and crystallization of amorphous food model. *J. Food Sci.* 56, 38-43.

Roos, Y. H., Karel, M., 1991c. Phase transitions of mixtures of amorphous polysaccharides and sugars. *Biotechnol. Progr.* 7(1), 49-53.

Roos, Y., 1993. Melting and glass transitions of low molecular weight carbohydrates. *Carbohydr. Res.* 238, 39-48.

Ruby, A. J., Kuttan, G., Babu, K. D., Rajasekharan, K. N., Kuttan, R., 1995. Anti-tumour and antioxidant activity of natural curcuminoids. *Cancer Lett.* 94 (1), 79-83.

Saffari, M., Ebrahimi, A., Langrish, T., 2016. A novel formulation for solubility and content uniformity enhancement of poorly water-soluble drugs using highly-porous mannitol. *Eur. J. Pharm. Sci.* 83, 52-61.

Salazar, J., Müller, R. H., Möschwitzer, J. P., 2014. Combinative particle size reduction technologies for the production of drug nanocrystals. *J. Pharm. (Cairo)* 2014, 265754.

Saleki-Gerhardt A., Zografi, G., 1994. Non-isothermal and isothermal crystallization of sucrose from the amorphous state. *Pharm. Res.* 11, 1166–1173.

Satoh, T., Hidaka, F., Miyake, K., Yoshiyama, N., Takeda, K., Matsuura, T., Imanaka, H., Ishida, N., Imamura, K., 2016. Surfactant-free solid dispersion of fat-soluble flavour in an amorphous sugar matrix, *Food Chem.* 197, 1136–1142.

Schebor, C., Mazzobre, M. F., Buera, M. D., 2010. Glass transition and time-dependent crystallization behavior of dehydration bioprotectant sugars. *Carbohydr. Res.* 345(2), 303-308.

Schenck, L., Lowinger, M., Troup, G. M., Li, L., McKelvey, C., 2019. Achieving a hot melt extrusion design space for the production of solid sollutions. In: Mary T. Ende D. J. eds. *Chemical Engineering in the Pharmaceutical Industry*, Beverly, Wiley-Scrivener Publishing, pp 469-487.

Sekikawa, H., Fujiwara, J., Naganuma, T., Nakano, M., Arita, T., 1978. Dissolution behaviors and gastrointestinal absorption of phenytoin in phenytoin-polyvinylpyrrolidone coprecipitate. *Chem. Pharm. Bull. (Tokyo)* 26 (10), 3033-3039.

Sekitoh, T., Okamoto, T., Fujioka, A., Tramis, O., Takeda, K., Matsuura, T., Imanaka, H., Ishida, N., Imamura, K., 2021a. Sole-amorphous-sugar-based solid dispersion of

curcumin and the influence of formulation composition and heat treatment on the dissolution of curcumin. *Dry. Technol.* 39 (14), 2065-2074.

Sekitoh, T., Okamoto, T., Fujioka, A., Yoshioka, T., Terui, S., Imanaka, H., Ishida, N., Imamura, K., 2021b. Crystallization characteristics of amorphous trehalose dried from alcohol. *J. Food Eng.* 292, 110325.

Shah, D. A., Murdande, S. B., Dave, R. H., 2016. A review: Pharmaceutical and pharmacokinetic aspect of nanocrystalline suspensions. *J. Pharm. Sci.* 105, 10-24.

Sher, P., Insavle, G., Porathnam, S., Pawar, A. P., 2007. Low density porous carrier drug adsorption and release study by response surface methodology using different solvents. *Int. J. Pharm*. 331, 72–83.

Shimada, Y., Roos, Y., Karel, M., 1991. Oxidation of methyl linoleate encapsulated in amorphous lactose-based food model. *J. Agric. Food Chem.* 39, 637-641.

Shivanand, P., Sprockel, O. L., 1998. A controlled porosity drug delivery system. *Int. J. Pharm*. 167, 83–96.

Sinha, B., Müller, R. H., Möschwitzer, J. P., 2013. Bottom-up approaches for preparing drug nanocrystals: formulations and factors affecting particle size. *Int. J. Pharm.* 453 (1), 126-141.

Singh, A., Van den Mooter, G., 2016., Spray drying formulation of amorphous solid dispersions. *Adv. Drug Deliv. Rev.* 100, 27-50.

Slade, L., Levine, H., 1988. Non-equilibrium behavior of small carbohydrate-water system. *Pure & Appl. Chem.* 60, 1841-1864.

Slade, L., Levine, H., 1991. Beyond water activity: recent advances based on an alternative approach to the assessment of food quality and safety. *Crit. Rev. Food Sci. Nutr.* 30, 115-360.

Sobue, S., Tan, K., Shaw, L., Layton, G., Hust, R., 2004. Comparison of the pharmacokinetics of fosfluconazole and fluconazole after single intravenous administration of fosfluconazole in healthy Japanese and Caucasian volunteers. *Eur. J. Clin. Pharmacol.* 60 (4), 247-253.

Sriraman, S. K., Torchilin, V. P., 2014. Recent advances with liposomes as drug carriers. In: Ashutosh T. Anis N. eds. *Advanced Biomaterials and Biodevices*, Beverly: Wiley-Scrivener Publishing, pp 79-119.

Stella, V. J., Charman, W. N., Naringrekar, V. H., 1985. Prodrugs. Do they have

advantages in clinical practice? *Drugs* 29 (5), 455-473.
Stella, V. J., 2004. Prodrugs as therapeutics. *Expert Opin. Ther. Pat.* 14 (3), 277-280.
Stella, V. J., 2007. A Case for prodrugs. In: Stella, V. J., Borchardt, R. T., Hageman, M. J., Oliyai, R., Maag, H., Tilley, J. W., eds. *Prodrugs: Challenges and Rewards Part 1*, NewYork: Springer New York, pp 3-33.
Stella, V. J., 2010. Prodrugs: Some thoughts and current issues. *J. Pharm. Sci.* 99 (12), 4755-4765.
Sun, D., Lee, PI., 2010. Evolution of supersaturation of amorphous pharmaceuticals: The effect of rate of supersaturation generation. *Mol. Pharm.* 10, 4330-4346.
Surana, R., Pyne, A., Suryanarayanan, R., 2004. Effect of preparation method on physical properties of amorphous trehalose. *Pharm. Res.* 21, 1167-1176.
Sutton, S. C., Evans, L. A., Fortner, J. H., McCarthy, J. M., Sweeney, K., 2006. Dog colonoscopy model for predicting human colon absorption. *Pharm. Res.* 23, 1554–1563.
Suzuki, H., Sunada, H., 1998. Influence of water-soluble polymers on the dissolution of nifedipine solid dispersions with combined carriers. *Chem. Pharm. Bull.* 46, 482-487.
Takeda, K., Gotoda, Y., Hirota, D., Hidaka, F., Sato, T., Matsuura, T., Imanaka, H., Ishida, N., Imamura, K., 2017. Surfactant-free solid dispersions of hydrophobic drugs in an amorphous sugar matrix dried from an organic solvent. *Mol. Pharm.* 14(3), 791-798.
Takeda, K., Sekitoh, T., Fujioka, A., Yamamoto, K., Okamoto, T., Matsuura, T., Imanaka, H., Ishida, N., Imamura, K., 2019. Physical stability of an amorphous sugar matrix dried from methanol as an amorphous solid dispersion carrier and the influence of heat treatment. *J. Pharm. Sci.* 108 (6), 2056-2062.
Tant, M. R., Wilkes, G. L., 1981. An overview of the nonequilibrium behavior of polymer glasses. *Polym. Eng. Sci.* 21, 874–895.
Taylor, L. S., Zografi, G., 1997. Spectroscopic characterization of interactions between PVP and indomethacin in amorphous molecular dispersions. *Pharm. Res.* 14, 1691-1698.
Taylor, L. S., Zografi, G., 1998. Sugar-polymer hydrogen bond interactions in lyophilized amorphous mixtures. *J. Pharm. Sci.* 87, 1615–1621.
Taylor, L. S., Zhang, G. G. Z., 2016. Physical chemistry of supersaturated solutions and implications for oral absorption. *Adv. Drug Deliv. Rev.* 101, 122-142.
Thayer, A. M., 2010. Finding solutions. *Chem Eng News* 88, 13-18.
Thombre, A. G., Caldwell, W. B., Friesen, D. T., McCray, S. B., Sutton, S. C., 2012. Solid

nanocrystalline dispersions of ziprasidone with enhanced bioavailability in the fasted state. *Mol. Pharm*. 9, 3526-3534.

Torchilin, V. P., 2005. Recent advances with liposomes as pharmaceutical carriers. *Nature Rev. Drug Discovery* 4, 145–160.

Tramis, O., Fujioka, A., Imanaka, H., Ishida, N., Imamura, K., 2022. Spontaneous foaming during vacuum drying of polyvinylpyrrolidone- and sugar-alcohol mixtures and enhancement of water-dissolution of water insoluble drug. *Dry. Technol.* 40(3), 604-614.

Tsourouflis, S., Flink, J. M., Karel, M., 1976. Loss of structure in freeze carbohydrate solutions: effect of the temperature, moisture content and composition. *J. Sci. Food Agric.* 27, 509-519.

Wadke, D. A., Serajuddin, A. T. M., Jacobson, H., 1989. Preformulation testing. In: Lieberman, H. A., Lachman, L., Schwartz, J.B., eds. *Pharmaceutical Dosage Forms: Tablets*. New York : Marcel Dekker, Vol. 1, p 1–73.

Walters, R. H., Bhatnagar, B., Tchessalov, S., Izutsu, H., Tsumoto, K., Ohtake, S., 2014. Next generation drying technologies for pharmaceutical applications. *J. Pharm. Sci*. 103, 2673-2695.

Weuts, I., Kempen, D., Vereck, G., Peeters, J., Brewster, M., Blaton, N., van den Mooter, G., 2005. Salt formation in solid dispersions consisting of polyacrylic acid as a carrier and three basic model compounds resulting in very high glass transition temperatures and constant dissolution properties upon storage. *Eur. J. Pharm. Sci.* 25, 387-393.

Won, D. H., Kim, M. S., Lee, S., Park, J. S., Hwang, S. J., 2005. Improved physicochemical characteristics of felodipine solid dispersion particles by supercritical anti-solvent precipitation process. *Int. J. Pharm.* 301 (1-2), 199-208.

Wu, L., Orikasa, T., Ogawa, Y., Tagawa, A., 2007. Vacuum drying characteristics of eggplants. *J. Food Eng.* 83(3), 422–429.

Yadav, B. V., Yadav, A. V., 2009. Pharmaceutical application of supercritical fluid technique: an overview. *J. Pharm. Res.* 29, 31-44.

Yu, J. Y., Kim, J. A., Joung, H. J., Ko, J. A., Park, H. J., 2020. Preparation and characterization of curcumin solid dispersion using HPMC. *J. Food Sci.* 85 (11), 3866-3873.

Yu, L., 2001. Amorphous pharmaceutical solids: Preparation, characterization and stabilization. *Adv. Drug Deliv. Rev.* 48 (1), 27-42.

Zhao, X., Wang, G., Zhang, B., Li, H., Nie, Q., Zang, C., Zhao, X., 2009. Development of Silymarin nanocrystals lyophilized power applying nanosuspension technology. *Zhongguo Zhong Yao Za Zhi* 34 (12), 1503-1508.

Zhou, Y., Roos, Y. H., 2012. Stability and plasticizing and crystallization effects of vitamins in amorphous sugar systems. *J. Agric. Food Chem.* 60(4), 1075-1083.

Zhuo, K., Zhang, H., Wang, Y., Liu, Q., Wang, J., 2005. Activity coefficients and volumetric properties for the NaBr + maltose + water system at 298.15 K. *J. Chem. Eng. Data* 50, 1589-1595.

List of Publications

(1) Takeda, K.; Gotoda, Y.; Hirota, D.; Hidaka, F.; Sato, T.; Matsuura, T.; Imanaka, H.; Ishida, N.; Imamura, K., Surfactant-Free Solid Dispersions of Hydrophobic Drugs in an Amorphous Sugar Matrix Dried from an Organic Solvent. *Mol. Pharm.* **2017,** *14* (3), 791-798.

(2) Takeda, K.; Sekitoh, T.; Fujioka, A.; Yamamoto, K.; Okamoto, T.; Matsuura, T.; Imanaka, H.; Ishida, N.; Imamura, K., Physical Stability of an Amorphous Sugar Matrix Dried From Methanol as an Amorphous Solid Dispersion Carrier and the Influence of Heat Treatment. *J. Pharm. Sci.* **2019,** *108* (6), 2056-2062.

(3) Takeda, K.; Miyazaki S.; Okamoto, T.; Imanaka, H.; Ishida, N.; Imamura, K., Water Sorption and Glass-to-Rubber Transition Characteristics of Amorphous Sugar Matrices, Dried from Alcohols under different Conditions. *J. Food Eng.* **2023**, *349,* 111483.

Acknowledgment

The author wishes to express my sincerest gratitude to Professor Koreyoshi Imamura for his kind guidance, valuable suggestions, and critical discussions throughout this work. The author learned important attitudes and thinking as a researcher from his kind and strict instruction.

I would like to thank the thesis reviewing committee, Professor Tsutomu Ono and Associate Professor Koichi Nakaso, for their valuable comments and insightful suggestions for my thesis.

I wish to express my sincere gratitude to Professor Naoyuki Ishida and Assistant Professor Hiroyuki Imanaka for their valuable suggestions and encouragement.

I am thankful to Technical Staff, Mrs. Yukiko Kurimoto, for her great support. Thanks are due to all members and graduates of Professor Imamura's laboratory. The author couldn't complete the study without their encouragement and mental support. In particular, I am grateful to Mr. Tomo Sato, Mr. Fumihiro Hidaka, Mr. Daichi Hirota, Mr. Yuto Gotoda, Ms. Akiho Fujioka, Mr. Takanari Sekitoh, Ms. Kayoko Yamamoto, Mr. Takashi Okamoto, Mr. Shinta Miyazaki for their great effort to the study.

I gratefully acknowledge the Suga Hiroaki, Murakami Hiroshi scholarship received from Okayama University and JST SPRING, Grant Number JPMJSP2126.

Finally, the author expresses his appreciation to his parents Mr. Kazuo Takeda, and Mrs. Yoshie Takeda, for their kind support.

Koji Takeda